**M-Pos554**

**OVEREXPRESSION OF mu MDR 1 PROTEIN INHIBITS $Na^+$-INDEPENDENT $Cl^-/HCO_3^-$ EXCHANGE IN TRANSFECTED CHINESE HAMSTER OVARY CELLS** ((John Gately Luz, Li-Yong Wei, Subham Basu & Paul D. Roepe)) Program in Molecular Pharmacology & Therapeutics, Memorial Sloan-Kettering Cancer Center and Graduate School of Medical Sciences Cornell University 1275 York Avenue, New York, New York 10021.

We have measured intracellular pH ($pH_i$) for multidrug resistant (MDR) cell lines constructed by transfecting LR73 fibroblasts with mutant and wild type murine MDR 1 genes. Plasma membrane electrical potential ($\Delta\Psi$) has also been measured by the $K^+$/valinomycin null point titration method using the ratiometric probe di-4-ANEPPS. Both the untransfected, parental cell line and a cell line expressing substantial mutant MDR 1 protein (K432R/K1074R) that is unable to confer the MDR phenotype are found to have $\Delta\Psi \geq -40$ (±5) mV and $pH_i \leq 7.16$ (± 0.03) units. In constrast, MDR cell lines constructed by transfecting wild type mu MDR 1 cDNA are found to exhibit $\Delta\Psi$ 15 - 19 mV lower and $pH_i$ from 0.13 to 0.34 units higher. Northern and western blot analyses confirm the substantial overexpression of the mu MDR genes and proteins in these lines, as well as the mild overexpression of endogenous hamster pGP mRNA in some lines. In general agreement with previous mass cell population studies that examined myeloma cells overexpressing hu MDR 1 protein (Roepe, P.D. *et al., Biochemistry* in the press) we find that the overexpression of wild type mu MDR 1 protein inhibits $Cl^-$ and $HCO_3^-$ - dependent $pH_i$ homeostasis. Via single cell photometry studies we now conclude that this is due to specific inhibition of $Na^+$ - independent $Cl^-/HCO_3^-$ exchange (strict anion exchange or AE). Decreased AE activity is not due to decreased expression of the exchanger. In fact, again similar to previous work we find *increased* levels of AE mRNA in some MDR cell lines. Several models that explain these data that are also consistent with the known physiology of cells that endogenously express MDR protein are suggested. These data are consistent with a model for MDR protein function wherein overexpression of the protein decreases $\Delta\Psi$ and/or elevates $pH_i$ via $Cl^-$ - and $HCO_3^-$ - dependent mechanisms.

*Supported by grants from the Raymond & Beverly Sackler Foundation, the Society of Sloan-Kettering, and a Cancer Center Support Grant (NCIP30CA08748). PDR is a Sackler Scholar at MSKCC.*

**M-Pos555**

**DETERGENT-MEDIATED SOLUBILIZATION OF P-GP CONTAINING MEMBRANES FROM MULTIDRUG RESISTANT CELLS**

((M. Garrigos and S. Orlowski)) SBPM, DBCM/CEA, CE Saclay, F-91191 Gif/Yvette Cédex, France (Spon. by M. le Maire)

Overexpression of the glycoprotein P-gp in plasma membrane of tumor cells is responsible for their resistance to a large number of structurally unrelated cytotoxic drugs. The resistance results from a hyperefflux of the drugs out of the cells and seems to be related to an ATP-dependent transport via the P-gp. To confirm this last point, it is necessary to reconstitute purified P-gp into liposomes. To this aim, a preliminary step is detergent-mediated membrane solubilization. We have used vesicles of purified total membranes from Chinese Hamster lung fibroblasts highly resistant to actinomycin D (DC-3F/ADX) to compare the efficiency in preserving P-gp ATPase activity of the following detergents: CHAPS, deoxycholate, C12E8, Triton X100, octylglucoside and dodecylmaltoside. Solubilization was conducted in PBS buffer pH=7.5, 20°C, with successive additions of detergent over a concentration range covering three decades, and monitored using both light scattering and sedimentation experiments. For all six detergents tested, P-gp ATPase activity decreases monotonously for increasing but still non-solubilizing detergent concentrations, and only CHAPS, at solubilization, is able to restore P-gp ATPase activity to its initial value. In all cases ATPase activation by verapamil is lost. Size exclusion liquid chromatography on detergent equilibrated TSK SW 3000 column shows that after a centrifugation at 100.000 x g for 1 h the supernatant of CHAPS solubilized membranes contains P-gp mainly in an aggregated state, but still displaying ATPase activity.

## FUNCTIONAL IMAGING OF THE BRAIN

**Tu-AM-SymI-1**

COGNITIVE NEUROPHYSIOLOGY OF THE MOTOR CORTEX: STUDIES WITH SINGLE CELL RECORDINGS IN THE MONKEY. (A.P. Georgopoulos). Brain Sciences Center, Veterans Affairs Medical Center, Minneapolis, MN 55417.

Some principles underlying the representation and processing of directional information in the motor cortex will be discussed in this presentation. Large populations of neurons in motor cortex are engaged with reaching movements. This engagement is fairly early, starting approximately 60 ms following target onset. The intensity of cell discharge is modulated with the direction of reaching. Typically, the firing rate is a sinusoidal function of the direction. An unambiguous, distributed code for direction exists in neuronal populations in the motor cortex. The outcome of this population code can be visualized as a vector that points in the direction of the upcoming movement ("neuronal population vector"). The neuronal population vector has the following properties: it is an accurate and robust predictor of direction; it is resistant to cell loss; it can be estimated reliably from about 100-150 cells; it predicts well the direction during the reaction time, well before the motor output begins; it predicts the direction of reaching during an instructed delay period, in the absence of immediate motor output; and it predicts the direction of reaching during reaching in memorized directions, that is in the absence of a target. Finally, when a mental transformation is required for the generation of a reaching movement in a different direction from a reference direction, the population vector can provide useful information concerning the nature of the cognitive process by which the required transformation is achieved (Georgopoulos et al.: Mental rotation of the neuronal population vector. *Science* 243:234-236, 1989).

**Tu-AM-SymI-2**

MAGNETIC SOURCE IMAGING OF HUMAN BRAIN FUNCTIONS. ((S.J. Williamson)) Neuromagnetism Laboratory, Department of Physics and Center for Neural Science, New York University, New York, NY 10003.

The advent of large arrays of superconducting detectors now makes it possible to characterize the spatio-temporal dynamics of neural activity of the human brain from measurements of the magnetic field pattern near the scalp. The wide-band response of these sensors provides millisecond resolution in quantitatively defining the strength of local activity in the cerebral cortex. Our studies of two regions in the auditory cortex separated by only 1 cm reveal different dynamical features in primary and association areas which characterize distinct properties of sensory memories. These non-invasive 'physiological' studies of neural activity accurately predict the lifetime of auditory sensory memory (echoic memory) for individual human subjects. While the magnetic inverse problem provides no unique solution, it is nevertheless possible to obtain best estimates for the spatial distribution of intracellular electric currents. Such a magnetic source image (MSI) can account for the sources of magnetic field power, as well as the covariance between sources at different locations. Consequently, the magnetic observation of localized suppression of spontaneous rhythms, such as those in the alpha bandwidth, can be interpreted as desynchronization of cortical activity in specific anatomical areas, as when they become engaged in a sensory or cognitive task. By these methods, the rapid response of magnetic sensors can be exploited to characterize the fast-paced evolution of neural activity in various regions of the brain.

**Tu-AM-SymI-3**

FUNCTIONAL MAPPING OF THE HUMAN BRAIN WITH POSITRON TOMOGRAPHY ((RSJ Frackowiak)) MRC Cyclotron Unit, Hammersmith Hospital, London W12 0HS, UK

Positron emission tomography is a radiotracer based technique which capitalises on back projection reconstruction algorithms to provide quantitative distributions of cerebral perfusion in the human brain non-invasively in life. Measurements of the distribution of perfusion can be recorded in various experimental and control states and comparisons can be made between them. Local cerebral perfusion is an index of local synaptic firing and hence perfusion mapping provides a means of understanding the anatomical substrate of various cortical and subcortical functions. The lecture will illustrate the principles of the technique and the information that can be obtained by reference to studies in the visual system.

**Reference**

Zeki S, Watson JDG, Lueck CJ, Friston KJ, Kennard C, Frackowiak RSJ. J Neurosci 1991;11:641-649.

Watson JDG, Myers R, Frackowiak RSJ, Hajnal V, Woods RP, Mazziotta JC, Shipp S, Zeki S. Cereb Cortex 1993;3:79-94.

**Tu-AM-SymI-4**

FUNCTIONAL BRAIN MAPPING WITH MAGNETIC RESONANCE IMAGING: RECENT DEVELOPMENTS AND ACCOMPLISHMENTS (Kâmil Uğurbil, University of Minnesota, Center for Magnetic Resonance Research, Minneapolis, MN)

The study of the human brain requires methods of delineating regions of neuronal activity during performance of various tasks. A new magnetic resonance imaging (MRI) method has been shown to provide functional maps of the human brain using BOLD (Blood Oxygen Level Dependent) contrast. BOLD has its origin in the magnetic properties of hemoglobin and was first observed at high magnetic fields (Ogawa, et al: (1990) Magn. Reson. Med. 14:68). Functional imaging with MRI is based on BOLD effect and the hemodynamic and metabolic response of the brain to increased neuronal activity.

Functional MRI has already been utilized to study sensory stimulation, motor task, and cognitive processes in humans. In this lecture, the present accomplishments, the potential and the limitations of the BOLD MRI functional imaging will be reviewed and discussed.

**Tu-AM-A1**

CALMODULIN CANNOT EFFECTIVELY REPLACE TROPONIN C. ((F. Schachat, S. George*, and P.W. Brandt‡)) Cell Biology and *Medicine, Duke University Medical Center, Durham, NC 27710 and ‡Anatomy and Cell Biology, Columbia University Medical School, New York, NY 10032

In vitro studies on troponin C (TnC) show that, in the presence of $Ca^{2+}$, it can partially activate several of the cytosolic enzymes normally regulated by $Ca^{2+}$-calmodulin (CaM). Here we investigate the extent to which calmodulin can function as a TnC. Early studies suggested that CaM was unable to substitute for TnC, but as demonstrated by Gulati and Babu, that was due largely to calmodulin's inability to bind to thin filaments at the low [$Ca^{2+}$] characteristic of relaxed muscle. This observation led to the proposal that CaM would be a fully competent TnC replacement, if it were stably associated with the thin filament. We have tested this possiblity by using a CaM/3,4TnC chimera in which the low affinity $Ca^{2+}$-specific domains III and IV in CaM a replaced by the homologous high affinity divalent metal ion binding domains of cardiac TnC. Substitution of these domains enabled CaM/3,4TnC to bind TnC-extracted fibers at low $Ca^{2+}$ in the presence of $Mg^{2+}$. Despite its stable association with the thin filament, the CaM/3,4 TnC chimera is no better able to generate maximal tension than CaM. Moreover, the CaM/3,4 TnC substituted fibers exhibit significiantly reduced $Ca^{2+}$-senstivity and little of the extended cooperativity of $Ca^{2+}$-activation observed in control fibers.

**Tu-AM-A2**

**NEBULIN-CALMODULIN AS A NEW CALCIUM REGULATORY SYSTEM ON THE THIN FILAMENT OF SKELETAL MUSCLE.** ((Douglas D. Root & Kuan Wang)) Department of Chemistry and Biochemistry, The Biochemical Institute and Cell Research Institute, University of Texas at Austin, Austin, Texas 78712. (Spon. by Dr. Joseph Starnes )

Nebulin is a giant protein ruler of the actin filament of skeletal muscle. This modular protein consists primarily of a repeating sequence (module) of 35 residues and a super-repeat of seven modules. These modules are thought to be actin binding domains along the length of nebulin. Cloned nebulin fragments of 6-8 modules bind with high affinity to actin, myosin, and myosin subfragment S-1. These fragments bound at a ratio of 1-2 nebulin fragments per actin monomer with high affinity as determined by cosedimentation binding assays. Through cosedimentation assays, fluorescent microscopy, and solid-phase binding assays, we have also observed the binding of nebulin fragments to myosin and the chymotryptic myosin subfragment S-1. Binding to myosin rod was not detected. This data indicates that nebulin can bind both to actin filaments and the head of myosin and suggests that nebulin might play a role in the regulation of actomyosin interactions. These observations raised the intriguing possibility that nebulin might have regulatory functions on actomyosin interactions. Nebulin fragments from the overlap region of the sarcomere inhibited actomyosin ATPase activities and sliding velocities of actin over myosin in motility assays. Calmodulin reversed the inhibition and accelerated actin sliding in a calcium dependent manner. The data suggest that the nebulin-calmodulin system responds to calcium by increasing actin sliding over myosin in activated muscle and by preventing sliding and actin-activated ATPase hydrolysis in resting muscle. Nebulin may function as a thin filament regulatory protein.

**Tu-AM-A3**

**Elimination of Charged Residue Clusters in Subdomain-1 of Yeast Actin Decreases Its Affinity to Myosin But Does Not Prevent Sliding Over HMM in the *In Vitro* Motility Assays** ((C.Miller and E.Reisler)) Department of Chemistry and Biochemistry and Molecular Biological Institute, UCLA CA 90024

Yeast actin mutants with alanines replacing charged amino acid clusters D24/D25, E99/E100, D80/D81 or E83/K84 were studied to assess their role in interactions with myosin. In a previous report *Dictyostelium* actin filaments with residues D24/D25 or E99/E100 replaced with histidines showed complete or partial loss of filament sliding in the *in vitro* motility assay (Johara *et al*,PNAS March 93). In contrast to this, inclusion of 0.5% methylcellulose to the motility assay buffer allowed filaments with alanines substituted at D24/D25 or E99/E100 to move with sliding velocities of 3.3$\mu$m/s and 3.9 $\mu$m/s, respectively, compared to 3.2$\mu$m/s for the wildtype. In the absence of methylcellulose mutant filaments were dissociated from the assay surface by MgATP while wildtype filaments moved at 3.4 $\mu$m/s. This indicates a lower affinity of S1.ATP for the mutants than for wildtype actin. Alanine mutants at D80/D81 and E83/K84 had sliding velocities of 3.9 $\mu$m/s and 3.6 $\mu$m/s, respectively, compared to 3.8 $\mu$m/s for wildtype. Co-sedimentation of actin filaments with S-1 in the presence of ATP-$\gamma$-S showed a 75% and 55% decrease in the binding of D24/D25 and E99/E100 mutant actins to S1 respectively, relative to that of wildtype. Measurement of the actin-activated ATPase showed large decreases in the activation of S-1 for D24/D25 and E99/E100 mutants compared to wildtype actin.

**Tu-AM-A4**

ASSESSMENT OF THE ROLE OF MYOSIN REGULATORY LIGHT CHAIN (MRLC) PHOSPHORYLATION BY *IN VIVO* MUTAGENESIS IN *DROSOPHILA*. ((H. Yamashita[1], R. Tohtong[3], A. Simcox[3], J. Vigoreaux[2], J. Haeberle[1], C. Hyatt[1], S. Brown[1], and D. Maughan[1])) [1]Dept. Molecular Physiology & Biophysics, [2]Dept. Zoology, University of Vermont, Burlington, VT 05405, and [3]Dept. Molecular Genetics, Ohio State University, Columbus, OH 43210.

*Drosophila* muscle-specific MRLC is phosphorylated at Ser66 and Ser67 by calcium-activated calmodulin and myosin light chain kinase. To investigate the significance of MRLC phosphorylation on contractile function *in vivo*, Ser66 and/or Ser67 were changed to unphosphorylatable Ala (S66A and/or S67A) by P-element mediated germline transformation. The flight ability and wing beat frequency was reduced in double mutants (S66A,S67A) and S66A single mutants as compared with the control, while S67A single mutants mimicked the control. The mechanical performance of isolated indirect flight muscle (IFM) fibers was studied by sinusoidal analysis. In double mutants, the maximum power output (P) and the frequency at which the power output was maximum (fmax) decreased by one tenth and by half, respectively, as compared with the control. Although in single mutants (S66A or S67A) both P and fmax were intermediate between the double mutants and the control, the reduction was larger in S66A than S67A. Thus, phosphorylation of Ser66 may be more important than Ser67 for normal flight ability, suggesting that the phosphorylation site on MRLC conserved throughout species may be Ser66, and that phosphorylation of Ser67 may have an additive role for normal contractile function in *Drosophila* IFM. Supported by NIH AR40234.

**Tu-AM-A5**

POSTTRANSLATIONAL REGULATION OF THE ALKALI MYOSIN LIGHT CHAIN RATIOS IN ADULT SKELETAL MUSCLE ((F. Schachat, E.K. Williamson, and M. Maready)) Cell Biology, Duke University Medical School, Durham, NC 27710.

Fast alkali myosin light chains (mlc-1f and mlc-3f) are generated from the same gene by alternative splicing. Studies during fetal development show that expression of the alkali mlcs is transcriptionally-regulated. We find the situation in adult muscle is different. mlc-1f is the predominant alkali light chain in adult fast muscles, present in molar ratios to mlc-3f that range from 1.5 to 3.5. But, pulse labelling studies indicate that mlc-3f is synthesized and incorporated into myofibrils at approximately 1.5x the rate of mlc-1f. Both RNA-PCR and *in vitro* translation experiments show that the synthetic ratios of the mlcs reflect the steady-state levels of their mRNAs. Thus the difference between their translational and accumulation ratios must be posttranslationally controlled. The absence of a significant sarcoplasmic pool of alkali mlcs, coupled with slow rate at which the steady-state ratios are reached, suggests that differential turnover is the most likely explanation for the difference between the synthetic rates and accumulation ratios of the alkali mlcs.

**Tu-AM-A6**

MAPPING METHIONINE RESIDUES IN CARDIAC TROPONIN C UPON BINDING CALCIUM AND TROPONIN I PEPTIDE. ((J.W. Howarth, G.A. Krudy, X. Lin, J.A. Putkey and P. R. Rosevear)) Dept. Biochemistry and Molecular Biology, Univ. of Texas Medical School, Houston, TX 77225 (Spon. by P. Rosevear)

The paramagnetic relaxation reagent, 4-hydroxy-2,2,6,6-tetramethylpiperidinyl-1-oxy (HyTEMPO), was used to probe the surface exposure of methionine residues of cardiac troponin C (cTnC) in the absence and presence of $Ca^{2+}$ at site II, as well as in the presence of the troponin I inhibitory peptide (cTnIp). The methyl resonances of the 10 Met residues of cTnC were chosen as spectral probes since they are thought to play a role in both formation of the hydrophobic pocket and in the binding of cTnIp. Met residues have been assigned in the HSMQC spectrum of cTnC by mutagenesis and metabolic labeling with [$^{13}$C-methyl]-Met. Proton longitudinal relaxation rates ($R_1$'s) of the [$^{13}$C-methyl] groups were determined using a $T_1$-HSMQC pulse sequence. Solvent exposed Met residues exhibit increased relaxation rates from the paramagnetic effect of HyTEMPO. Relaxation rates in 2 $Ca^{2+}$ and $Ca^{2+}$ saturated cTnC, both in the presence and absence of HyTEMPO, permitted the topological mapping of the conformational changes induced by the binding of $Ca^{2+}$ to site II, the site responsible for triggering muscle contraction. The increased exposure to HyTEMPO of Met residues 45 and 81 upon binding $Ca^{2+}$ to site II is consistent with an opening of the hydrophobic pocket in the N-terminal domain. The binding of cTnIp to both 2 $Ca^{2+}$ and $Ca^{2+}$ saturated cTnC was shown to partially protect Met residues 120 and 157 from HyTEMPO as determined by a decrease in their measured $R_1$' values. These results suggest that cTnIp binds primarily to the C-terminal domain of cTnC.

**Tu-AM-A7**

THE ESSENTIAL LIGHT CHAIN IS REQUIRED FOR FULL FORCE PRODUCTION IN SKELETAL MUSCLE MYOSIN.
((P. VanBuren, G. Waller*, K. Trybus*, D. Warshaw, and S. Lowey*)) Univ. of Vermont, Burlington, VT *Brandeis Univ., Waltham, MA

It has been shown recently that vertebrate skeletal muscle myosin light chains (LC) are required for rapid movement of actin filaments in an *in vitro* motility assay (Lowey et al., 1993). Removal of the regulatory LC (RLC) decreased velocity by 65%. More strikingly, myosin without the essential LC (ELC) moved actin at only 1/6 the rate of whole myosin, without a concomitant decrease in actin activated ATPase. To further characterize these myosins' mechanical capabilities, the isometric force generated by LC-deficient myosin was measured. A fluorescently labeled actin filament was attached to an ultra-compliant (50-200nm/pN) glass microneedle, and the actin filament was brought into contact with a myosin-coated surface (VanBuren et al., in press). RLC-deficient myosin exerted the same force as whole myosin, as previously observed in fiber studies (Moss et al., 1982). In contrast, ELC-deficient myosin exhibited <50% the force of whole myosin. Reconstitution of this myosin, immobilized on the motility assay surface, with ELC restored force to near control levels. Myosin's enzymatic and mechanical activities can therefore be uncoupled in the absence of LC, with ELC removal having a more profound effect on both velocity and force. These results suggest that the heavy chain in the neck region cannot by itself efficiently transmit mechanical activity between myosin's motor domain and the rod, and that light chains are necessary to fully express myosin's mechanical capabilities.

**Tu-AM-A8**

SMOOTH, SKELETAL AND CARDIAC MUSCLE MYOSIN FORCE ASSESSED BY CROSS-BRIDGE MECHANICAL INTERACTIONS *IN VITRO*.
((D. Harris, N. Alpert & D. Warshaw)) (Intro.: B. Hamrell) Mol. Physiol. & Biophys., Univ. of Vermont, Burlington, VT 05405.

To determine if muscle myosin isozymes have different force producing capacities at the molecular level, mixtures of skeletal, V1 cardiac, V3 cardiac and smooth muscle myosin were tested in an *in vitro* motility assay in which fluorescently labeled actin filaments were observed moving over a myosin coated surface. Alone, each myosin moved actin filaments at velocities proportional to their actin activated ATPase rates over a 450 fold range. Mixtures of two myosins moved actin filaments at velocities between those of the faster and slower myosin. The relationship between actin filament velocity and the proportion of the two myosins depended upon the types of myosins present. Data were analyzed with a model (Warshaw et al., 1990) which assumes that: 1) the two myosins interact mechanically, 2) each myosin's force:velocity relationship (F:V) is continuous across zero force and 3) the *in vitro* myosin F:V is the same as that in the tissue from which the myosin was isolated. Results allow us to rank order the myosins by their average isometric force per cross-bridge (smooth > skeletal = V3 cardiac > V1 cardiac). The average force per cross-bridge varies by a factor of 6 among the myosins tested, possibly providing a molecular basis for the enhanced force generation predicted by muscle tissue results (Murphy et al., 1974; Alpert et al., 1992) and supporting recent *in vitro* myosin force measurements (VanBuren et al., in press).

**Tu-AM-A9**

MODULATION OF CALCIUM EXCHANGE WITH THE CALCIUM SPECIFIC SITES OF TROPONIN C.
((J.D. Johnson, R.J. Nakkula and L.B. Smillie)) Dept. of Med. Biochemistry, The Ohio State Univ. College of Med. and Dept. of Biochemistry, Univ. of Alberta.

Calcium (Ca) binding to the two N-terminal Ca specific binding sites on skeletal troponin C (TnC) regulate the contraction-relaxation cycle of skeletal muscle. The mutant TnC, F29W, and dansylaziridine labeled TnC (TnC-DANZ) undergo large fluorescence increases when Ca binds to their N-terminal Ca specific sites (half-max at pCa5.8). Calmidazolium (R24571) and the additional mutation of Met 82 to Gln (F29WM82Q) both increased Ca affinity ~4-fold (half-max at pCa 6.4). Stopped-flow studies using F29W, F29WM82Q, TnC-DANZ and Quin 2 fluorescence indicate that R24571 and the M82Q mutation decrease the rate of Ca dissociation from the Ca specific sites ~3.4-fold (from ~462 ± 84/s to ~138 ± 30/s) at 22°C. Ca association with F29W, F29WM82Q and TnC-DANZ was very rapid (1-2 x $10^8$ $M^{-1}s^{-1}$) at 4°C. These drug and mutation induced increases in Ca affinity occur solely from large decreases in Ca off-rate without an effect on Ca on-rate. Thus, Ca binds to the Ca specific sites of TnC as rapidly as it diffuses to the protein, consistent with the speed of skeletal muscle contraction. These studies point out the potential of drugs and/or site directed mutagenesis to alter the Ca sensitivity of TnC's Ca specific regulatory sites and to directly affect the rate of Ca exchange and the rate of rise and/or the rate of relaxation of muscle.

**Tu-AM-A10**

MYOSIN DOMINATES WIDE ANGLE OPTICAL SCATTERING BY SKELETAL MUSCLE
((Mark Sharnoff)) Department of Physics, University of Delaware, Newark, DE 19716-2570

A well-known formula indicates that the intensity of Rayleigh scattering by a globular protein species in dilute solution is proportional to its molar concentration and to the square of its molecular weight. If the formula were to hold well even for moderately concentrated, quasi-crystalline protein suspensions, one would expect crossbridges to be responsible for 50 to 60% of the Rayleigh scattering observed from skeletal muscle. A simple experiment has confirmed this expectation. An isolated skeletal fiber placed on the stage of a polarizing microscope was illuminated alternately by white light and by a horizontally polarized laser beam traveling at ca. 15° to the fiber axis. In white light the A bands stood out brightly in the otherwise dim image. Under laser illumination the fiber became visible mainly via Rayleigh-scattered light. Sarcomeric cross-striations could be discerned amidst the speckle caused by the illumination's coherence, and they became prominent as the fiber was stretched to reduce or eliminate overlap of thick with thin filaments. The brighter portions of the Rayleigh images corresponded in position to the A bands seen in white light. Cross-correlation analysis, carried out by scanning the images with a CCD camera, indicated that at least 54% of the wide angle scattering by a fiber stretched to striation spacing 3.9 μm originated in the A bands.

Supported by NSF.

## MEMBRANES AND RELATED SYSTEMS

**Tu-AM-B1**

**Hydrophobic hydration of carboxilic acids**

((M.L. San Román Zimbrón [1] , I.Ortega Blake[2])), [1]UAEM, Laboratorio de Ingeniería molecular [2]UNAM Instituto de Física, Laboratorio de Cuernavaca, Apdo. Postal 139-B, Cuernavaca, Mor., 62191, MEXICO.

The solubility of non polar solutes in water has an anomalous dependence with temperature, it presents a minimum instead of a monotonous increase. Several attempts have been made to explain such an interesting phenomenon; but the interpretations of the available experimental data lead to contradictory conclusions.

Clearly, a better understanding of the molecular mechanism is needed and molecular simulations can help to clarify the origin of the peculiar thermodynamic properties of this system.

In this work we have followed a global simulation scheme for the hydration of a flexible molecule of propionic acid. To do this, in an economical way, we constructed an *ab initio* derived MCHO potential which shows an excellent trasferability within the carboxilic acids.

In a previous work we analyzed the effect of the tail length in the hydration of carboxilic acids. Now we look into the effect introducing a flexible molecule to clarify its influence on the thermodynamic properties, as well as on the hydration shell structure from 285 K to 355 K. The radial distribution functions of water around the hydrocarbon tails show a difference on the hydration shell structure with temperature.

**Tu-AM-B2**

ELECTRIC FIELD INDUCED CHANGES IN THE ALIGNMENT OF $H_{II}$ TUBULES
((P.D.Osman and B.A.Cornell)) CSIRO, Sydney, Australia.

The effect of electric field on samples of dioleoyl phosphatidylethanolamine in the $H_{II}$ phase, aligned between glass coverslips, has been investigated by $^{31}P$ nuclear magnetic resonance (NMR). The electric field was applied perpendicularly to the plane of the slide and changes in the $^{31}P$ NMR spectra were observed. These changes are interpreted as arising from a reorientation of the alignment of the hexagonal tubules as a result of an interaction between the electric field and a discontinuous dielectric formed by the lipid-water complex.

**Tu-AM-B3**

THERMOSENSITIVE LIPOSOMES: RELEASE OF DOXORUBICIN BY BOVINE SERUM AND HUMAN PLASMA IN RELATION TO HYPERTHERMIA. ((M.H. Gaber, K. Hong, S-K. Huang and D. Papahadjopoulos)) Cancer Research Institute, University of California San Francisco, CA 94143-0128.

This report describes the optimization of the formulation for thermosensitive, Doxorubicin-containing liposomes. The rate of release of encapsulated Doxorubicin from liposomes of various compositions was followed by fluorometric assay under defined thermal conditions (37, 42 and 45°C). The rate of release was assayed in buffer and also in both calf serum and human plasma up to 50%. The results showed that bovine serum was 10 times more active than human plasma in enhancing Doxorubicin release. The release of Doxorubicin from the liposomes at 37°C in 50% bovine serum was 15 times more than in buffer and liposomes with high cholesterol content released Doxorubicin two times more than cholesterol deficient liposomes. Inclusion of a small percentage of distearoylphosphatidylethanolamine (DSPE) derivatized with polyethyleneglycol (PEG) protected the liposomes from interaction with bovine serum at the lower temperature, thus decreasing the undesired release of Doxorubicin at 37°C. The optimal composition for the maximal differential release between 37°C and 42°C was a mixture of dipalmitoyl phosphatidylcholine/hydrogenated soy phosphatidylcholine/cholesterol and PEG-PE at a molar ratio of 100:50:30:6. In experiments designed to study the mechanism causing the instability of liposomes in bovine serum, we found two different distinct release patterns in liposomes: a slow linear rise of release for fluid liposomes such as egg PC/CHOL (50:50), and fast exponential rise and reaching plateau within 5 minutes for rigid liposomes such as DPPC/HSPC/CHOL (50:50:100). One of the plasma components which induced fast release of rigid liposomes was identified as C3 complement and was activated by $Mg^{2+}$.

**Tu-AM-B4**

**CONFORMATION AND DYNAMICS OF DIACYLGLYCEROL IN PHOSPHATIDYLCHOLINE BILAYERS BY A COMBINED SOLID STATE NMR AND MOLECULAR DYNAMICS ALGORITHM.** ((Charles R. Sanders, II and James P. Schwonek)) Dept. of Physiology and Biophysics, Case Western Reserve University, Cleveland, Ohio 44106.

*sn*-1,2-Dimyristoyl glycerol (DMDAG) and sn-1,2-dimyristoyl-3-fluoro propanediol (DMFPD) were synthesized in acyl perdeuterated $(d_{27})_2$ and carbonyl $(^{13}C{=}O)_2$ labeled forms. These compounds were dispersed in magnetically orientable dimyristoylphosphatidylcholine bilayers (see *Biochem.* 31, 8898-8905, 1992 and *Biophys. J.* 58, 447-460, 1991) and solid state $^{13}C$ and $^{2}H$ NMR spectra were acquired to yield a combined total of about 20 quadrupolar couplings, dipolar coupling, and chemical shift anisotropies for each molecule. Qualitatively, differences between the two data sets indicate that the hydroxyl proton plays a key role in establishing the orientation of the glycerol backbone and the degree of *sn*-1 and *sn*-2 acyl chain inequivalence. In order to more quantitatively interpret the data set for DMDAG, molecular dynamics simulations were carried out for DMDAG placed within a simulated phosphatidylcholine bilayer (see *Biophys. J.* 65, 1207-1218). Over 100 2 nsec calculations were completed followed by back calculation of the NMR data to test for the ability of each simulation to reproduce the experimental data set. Three such simulations were successful in this regard. The results of these simulations will be presented and provide considerable insight into interfacial DMDAG including: conformational preferences, the degree of conformational flexibility, the orientation of the glycerol backbone, the near 0 $^{13}C$ chemical shift anisotropy of the sn-2 carbonyl carbon, and the possibility of intramolecular hydrogen bonding.

**Tu-AM-B5**

CALCIUM IONS AND THE INTERACTIONS OF HYDROPHOBIC LUNG SURFACTANT PROTEINS SP-B AND SP-C WITH PHOSPHOLIPIDS IN SPREAD MONOLAYERS. ((S. Taneva and K.M.W. Keough)) Departments of Biochemistry and Pediatrics, Memorial University of Newfoundland, St. John's, Newfoundland, Canada A1B 3X9

Films of SP-B and SP-C, and SP-B:SP-C (2:1, w/w), alone or mixed with dipalmitoylphosphatidylcholine (DPPC) and dipalmitoylphosphatidylglycerol (DPPG), were formed on 0.15 M NaCl, 0.002 M $CaCl_2$ subphases. Surface pressure ($\pi$)-area characteristics of the films of the proteins were the same as those in the absence of $Ca^{2+}$. Calcium did not affect the properties of films of SP-B, or SP-C, or SP-B:SP-C (2:1, w/w) with DPPC. The $\pi$-area isotherms for the mixed films of the proteins with DPPG were $Ca^{2+}$-dependent. Calcium decreased the exclusion pressures of the proteins from the protein-DPPG films in comparison to those in its absence. Calcium suppressed the ability of SP-C and SP-B:SP-C (2:1, w/w) to remove phospholipid from protein-DPPG films. The influence of $Ca^{2+}$ on the DPPG films, consistent with diminished lipid-protein interactions, may be due to the effects of $Ca^{2+}$ on the ionization state, molecular packing and head group hydration of DPPG. (Supported by the Medical Research Council of Canada.)

**Tu-AM-B6**

**EFFECTS OF CHOLESTEROL AND SP-C ON MODEL LUNG SURFACTANT BEHAVIOR.** ((V. Skita and S.G. Kavel)) Department of Biochemistry and Biomolecular Structure Analysis Center, Univ. Ct. Health Center, Farmington, CT 06030-2017.

Pulmonary surfactant is a complex mixture of phospholipids, neutral lipids, glycolipids, and protein at the alveolar air-liquid interface. It is composed primarily of phospholipid of which dipalmitoylphosphatidyl choline (DPPC) is the largest constituent. The surfactant monolayer functions to reduce the surface tension at the air-liquid interface at functional residual capacity (FRC), thus reducing the amount of work required to inflate the lungs. Structural information as to the conformation and interaction of the various components of the surfactant monolayer may lead to the development of better replacement compounds, as well as improve our basic understanding of how phospholipids and proteins behave at an air-liquid interface. In these studies, model surfactant composed of DPPC, dioleoylphosphatidyl glycerol (DOPG), cholesterol (CH), and surfactant protein-C (SP-C) were spread on a Langmuir trough. A physiological subphase (135 mM NaCl, 1 mM $CaCl_2$, 2 mM HEPES, pH 7.0) was used for all surface pressure ($\Pi$) measurements. Isotherms of $\Pi$ versus mean molecular area (mma) were collected as a function of mole fraction DPPC, $\chi$, ($\chi$ = = [DPPC]/([DPPC]+[DOPG])) for 0, 8, 17, and 25 M% CH. Studies of ternary or quaternary mixtures containing 10% (wt) SP-C or 10% (wt) SP-C and 17 M% CH respectively, were also done. We found that for ternary mixtures of DPPC:DOPG:CH, 17 and 25 M% CH condenses the phospholipid monolayer at a mma of 40 and 50Å$^2$. 8 M% CH condenses the monolayer at a mma of 40Å$^2$ and for $\chi > 0.5$ at 50Å$^2$. The monolayer expands for $\chi < 0.5$ at a mma of 50Å$^2$. At a mma of 90Å$^2$ a similar but smaller effect is observed. At a mma of 50Å$^2$, SP-C and CH both condense the monolayer to the same degree; at a mma of 40Å$^2$ however, the phospholipid:SP-C mixture approaches ideal mixing at $\chi > 0.7$. Surprisingly, 17 M% CH has very little effect on the phospholipid:SP-C mixtures. The authors would like to thank Dr. S. Hawgood of the Cardiovascular Research Institute, Univ. Ca. San Francisco, for providing SP-C. [Supported by NIH HL45284 and a Council for Tobacco Research Fellowship]

**Tu-AM-B7**

**INFLUENCE OF POLYETHYLENE GLYCOL AND AQUEOUS VISCOSITY ON ROTATIONAL DIFFUSION OF MEMBRANOUS Na,K-ATPASE.** ((M. Esmann, K. Hideg and D. Marsh)) Inst. of Biophysics, Univ. of Aarhus, Denmark; Central Lab. for Chemistry, Univ. of Pécs, Hungary; Max-Planck-Institut f. biophysik. Chemie, Göttingen, FRG. (Spon. G. Montich)

Rotational diffusion of spin-labelled membranous Na,K-ATPase from Squalus acanthias has been studied by saturation transfer electron spin resonance spectroscopy, as a function of the concentration of glycerol or polyethylene glycol (PEG) in the suspending medium. The rotational correlation time of the protein increases linearly with viscosity of the aqueous glycerol medium, with a gradient which indicates that ca. 50-70% of the volume of the Na,K-ATPase is external to the membrane. The rotational correlation times of the protein in PEG solutions are considerably greater than those in glycerol solutions of the same viscosity and increase nonlinearly with viscosity of the suspending medium, indicating that increasing concentrations of PEG induce aggregation of the integral proteins within the membrane. The value reached at 50% PEG (w/v) corresponds to a degree of aggregation of the proteins between 2 and 5 depending on whether the PEG polymer is excluded from the membrane surface region. The results are relevant to hydration forces and PEG-induced cell fusion.

**Tu-AM-B8**

CELLULAR FATTY ACIDS MODULATE MEMBRANE FLUIDITY AND LDL BINDING. ((E. Berlin, J. Hannah, K. Yamane, B.V. Howard)) Beltsville Human Nutrition Research Center, USDA, Beltsville, MD 20705 and Medlantic Research Institute, Washington, DC 20010.

We examined the effects of fatty acid composition on membrane fluidity and LDL binding in TR 715-19 cells, a CHO line which constitutively expresses the human LDL receptor. Steady state fluorescence anisotropy ($r_s$) was measured with DPH and its trimethylammonium (TMA-DPH) and propionic acid (DPH-PA) derivatives in cells grown in fatty acid supplemented media. Acid composition affected $r_s$ for DPH, but not for DPH-PA or TMA-DPH, thus limiting effects to the bilayer region.

| $r_s$ (37°C) | 16:0 | 18:0 | 18:1 | 18:2 | 20:5 | Control |
|---|---|---|---|---|---|---|
| DPH | .124 | .129 | .102 | .113 | .147 | .153 |
| DPH-PA | .221 | .224 | .227 | .222 | .232 | .225 |
| TMA-DPH | .253 | .252 | .241 | .229 | .245 | .247 |

Arrhenius plots for fluidity parameters, $(r_0/r - 1)^{-1}$, for DPH and DPH-PA were linear between 2 and 38°C but not for TMA-DPH. Cells enriched in 18:1 or 18:2 were the most fluid ($p<0.001$). Cellular enrichment in 16:0, 18:0, and 18:1 increased LDL receptor binding but, correlation between LDL binding and fluidity was weak ($r = 0.35$, $p = 0.06$). Hence, properties other than membrane fluidity must be involved in regulating LDL binding to its receptor.

Tu-AM-B9

## FLUORESCENCE STUDIES OF HEPARIN DYNAMICS AND ACTIVITIES ON BIOMIMETIC MEMBRANES

((Sun-Yung Chen and B. Wieb Van Der Meer)) Department of Physics and Astronomy, Western Kentucky University, Bowling Green, KY 42101.

A biomimetic membrane can be constructed by attaching biomolecules onto the surface of a polymeric membrane. With this type of membrane systems one is able to facilitate and/or enhance specific enzymatic functions of the biomolecules in a reusable fashion. Moreover, these membranes represent a model system for studying the structure-function relationship of the attached biomolecules. In this study, heparin, a well known and effective anticoagulant, was attached to the surface of an agarose matrix. Two different attaching modes were examined to compare their effects on heparin's biological activities. The dynamic parameters (e.g., bending and twisting rate) of the membrane-bound heparin were studied by steady-state and time-resolved fluorescence anisotropy measurements. Its anticoagulant activities (e.g., anti-thrombin and anti-Xa response) were measured spectroscopically. These parameters were correlated with each other in order to optimize the biological activity of heparin in a membrane environment.This work is supported by NSF (EHR-9108764).

## PHOTOSYNTHETIC REACTION CENTERS

Tu-AM-C1

### A COMPREHENSIVE RESONANCE RAMAN STUDY OF BACTERIAL PHOTOSYNTHETIC REACTION CENTERS.

((V. Palaniappan and David F. Bocian)) Department of Chemistry, University of California, Riverside, CA 92521.

Resonance Raman (RR) spectra have been obtained for photosynthetic bacterial reaction centers (RCs) by using a large number of excitation wavelengths in the range 337-900 nm that span the B-, $Q_X$- and $Q_Y$-bands. Spectra were obtained for quinone-reduced, special pair (P) oxidized and a variety of mutant RCs. The RR spectra of the RCs were compared with those of bacteriochlorophyll (BCh) and bacteriopheophytin (BPh) in solution, various model compounds and normal coordinate calculations. Based on this comparative analysis, a plausible set of assignments are proposed for the skeletal and carbonyl vibrations in the 1425-1760-$cm^{-1}$ region. Collectively, the vibrational data indicate the following: (1) the structures of the accessory bacteriochlorophylls ($BCh_L$ and $BCh_M$) are identical and similar to those of the five coordinate BCh in solution. (2) The structures of $P_L$ and $P_M$ are not identical and $P_M$ appears to be conformationally distorted relative to $P_L$. (3) The structures of L- and M-side bacteriopheophytins ($BPh_L$ and $BPh_M$)are alike for the most part and similar to those of BPh in solution; however, distinct structural differences between $BPh_L$ and $BPh_M$ arise due to the interaction of $C_9$=O keto group of $BPh_L$ with $Glu_{L104}$.

Tu-AM-C2

### A GENETIC SYSTEM FOR ANALYSIS OF THE PHOTOSYNTHETIC REACTION CENTER FROM *RHODOPSEUDOMONAS VIRIDIS*

((E. J. Bylina, J. Moulds, P. Silva and S. O'Neal)) Biotechnology Program, University of Hawaii at Manoa, Honolulu, HI 96822. (Spon. by M. Rayner)

While the highest resolution structural data (2.3Å) for the reaction center complex is available from *Rhodopseudomonas viridis* DSM133, a system for the expression of genetically modified reaction centers in this organism using non-photosynthetic growth modes is not available. We have characterized a heterotrophic strain of *Rps. viridis* which is being used to develop such a genetic system. The construction of a reaction center *puf* operon chromosomal deletion strain and a *puf* operon-containing complementing plasmid will be described. Genomic cosmid libraries of both our heterotrophic strain of *Rps. viridis* and *Rps. viridis* DSM133 were constructed. The entire *puf* operon is located on a 9 kb HindIII fragment in both strains. The structural genes encoding the β and α subunits of the light harvesting complex and the L, M, and cytochrome subunits of the reaction center will be deleted from the *Rps. viridis* chromosome by interposon mutagenesis. The broad host range plasmid pRK291 serves as the vector for our complementing plasmid. Unique and nonmutagenic restriction sites are being engineered into this plasmid to divide the *puf* operon into several regions. This system will be used for the construction of directed mutations throughout the *Rps. viridis* reaction center.
Supported by NIH grant GM48556, NSF grant MCB-9206080 and NIH-MBRS Grant GM08125-20.

Tu-AM-C3

### A LARGE SCALE SYMMETRY MUTANT IN THE RB.CAPSULATUS REACTION CENTER

((N.W. Woodbury, J.E. Eastman, H.M. Murchison))Department of Chemistry and Biochemistry, Arizona State University, Tempe, Az. 85287-1604

A large scale symmetry mutant,SYM 2-1, of the *Rb.capsulatus* reaction center was constructed containing a partial d-helix swap in which M subunit residues from M205 to M210 were replaced by the corresponding L amino acids.

Isolated reaction centers showed a steady state absorption spectrum largely unchanged from wild type (wt) in the presence of ionic strength greater than 100 mM. In ionic strenghth less than 100 mM however, an approximately 40 nm reversible blue shift of the special pair (P) Qy peak occurs. Further analyses showed that there is no pH dependence of the bandshift, but ionic detergents have an effect similar to that of salt. In addition to the bandshift of the Qy transition of P, the oscillator strength of the 1250 nm absorption associated with $P^+$ decreases by roughly five-fold at low ionic strength.

The standard free energy change between $P^*$and $P^+Bph_A^-$ decreased by 76 meV in SYM 2-1 at high ionic strength compared to wt as determined by time correlated single photon counting measurements of the thermal repopulation of $P^*$ after $P^+H_A^-$ formation. The $P/P^+$ oxidation potential of SYM 2-1 reaction centers was measured at low ionic strength and found to be only 24 meV above wt. No evidence was found that the two spectral forms of P in SYM 2-1 reaction centers had different $P/P^+$ oxidation potentials. As has been found for other high potential mutants, the $P^+Q_A^-$ recombination time was faster in the mutant in high ionic strength, increasing from 121 ms in wt to 42 ms.

Tu-AM-C4

### CHIMERIC MUTAGENESIS OF *RB. CAPSULATUS* REACTION CENTERS UTILIZING *C. AURANTIACUS* SEQUENCE: REPLACEMENT OF THE B-BRANCH MONOMER BACTERIOCHLOROPHYLL WITH BACTERIOPHEOPHYTIN.

((D.M. Gallo, A.K.W. Taguchi, N.W. Woodbury)) Department of Chemistry and Biochemistry and the Center for the Study of Early Events in Photosynthesis, Arizona State University, Tempe, AZ 85287-1604

A series of three mutants were designed to investigate stabilizing the replacement of the B-branch monomer bacteriochlorophyll ($B_B$) with a bacteriopheophytin (Bpheo) utilizing *C. aurantiacus* sequence. In the first mutant, CAR1.0, the B-branch monomer binding pocket of *Rb. capsulatus* was replaced with the homologous region from *C. aurantiacus*. The replacement contained the following changes: Val M171 → Glu, Pro M174 → Ala, Tyr M175 → His, Phe M178 → Lys, Ser M179 → Ala, His M180 → Leu. In CAR2.0, only His M180 was changed to a Leu, as in Bylina et al. (1990) *Biochem.* **29**, 6203. CAR3.0 contains the same mutations as CAR1.0, except His M180 is not changed. Both pigment extractions and HPLC analyses of the RCs indicate that the Bchl: Bpheo ratio is 1:1 for CAR1.0 and CAR2.0, and 2:1 for CAR3.0 and wild-type (wt). Room temperature absorption spectra of the RCs are consistent with the replacement of $B_B$ with a Bpheo. In CAR1.0 and CAR2.0, there, is a 50% decrease in oscillator strength of the Bchl monomer band and the appearance of a new transition at 785 nm. In addition, the oscillator strength of the $Q_X$ transitions of the Bpheo is increased with the concomitant decrease in the Bchl $Q_X$ transitions. The spectrum of CAR3.0, is essentially identical to wt. The new chromophore in CAR1.0 and CAR2.0 is termed Φ. Light-dark difference spectra of RCs and chromatophores indicate that the RCs can undergo primary electron transfer. Time-resolved absorption spectroscopy indicates that in CAR2.0, the rate of initial electron transfer is unchanged, however the NIR absorption changes upon the formation of the state $P^+Bpheo^-$ are significantly altered. Preliminary evidence also suggests that in CAR1.0, which contains five mutations in addition to the His M180 → Leu change, there is a fast, less than 1 ps quenching process acting upon the excited singlet state of P.

**Tu-AM-C5**

STABILIZATION OF BURIED CHARGES IN PHOTOSYNTHETIC REACTION CENTERS. ((M.R. Gunner, A. Joguine, Z.Dong, ))
Physics Dept. C.C.N.Y N.Y., NY 10031

The environment of the ionizable groups in bacterial photosynthetic reaction centers (RC) from Rps. viridis and Rb. sphaeroides are examined. A surprising number are deeply buried. In Rps. viridis RC (1PRC) DELPHI calculations show 37 ARG (58% of total), 7 LYS (21%), 23 ASP (49%) and 23 GLU (44%) have lost at least 5 Kcal solvation (reaction field) energy. Rb. sphaeroides RCs show a similar pattern. The charge states of these internal residues are modulated by protein structural elements, including: (1) salt bridges which stabilize the ionized form; (2) hydrogen bonds to water or sidechain hydroxyl groups, a motif that supports changes in ionization state; and (3) protein backbone dipoles oriented in helices and loops to produce regions of positive or negative potential. One function of the buried ionizable residues is seen in a cluster containing 12 acids and only 5 bases near $Q_B$ in both Rps. viridis and Rb. sphaeroides RCs. The arrangement is stabilized by backbone dipoles, which yield as much as 15 Kcal stabilization of the ionized acids. The cluster of acids appears to provide an internal buffer for proton transfer in the $Q_B$ pocket, contributing to the weak pH dependence of proton uptake following the first electron transfer, and to the surprising insensitivity of the protein function to certain mutations. Supported by GM48726-01.

**Tu-AM-C6**

ELECTRON TRANSFER $Q_A^-Q_B \rightarrow Q_AQ_B^-$ IN *RB. SPHAEROIDES*: POSSIBLE EVIDENCE FOR AN INTERMEDIATE STATE.* ((M.L. Paddock, M.S. Graige, G. Feher and M.Y. Okamura)) UCSD, Physics Dept. 0319, 9500 Gilman Dr., La Jolla, CA., 92093-0319, USA

Photoexcitation of the bacterial reaction center (RC) leads to electron transfer from the donor through a bacteriopheophytin and a primary quinone ($Q_A$) to a secondary quinone ($Q_B$). Kinetic measurements were made at 1°C in isolated RCs at 410nm ≤ λ ≤ 500nm, a range where $Q^-$ in solution has absorption peaks at 420nm and 450nm. The spectrum (see figure) of the kinetic phase ($k \geq 1000\ s^{-1}$) resembles that expected for the electron transfer $Q_A^-Q_B \rightarrow Q_AQ_B^-$ where $Q_A^-$ and $Q_B^-$ have slightly shifted absorbance peaks. The positive peak at ~ 440nm indicates the creation of a semiquinone at a rate $k \sim 3300\ s^{-1}$ (± 10 %). The negative peak at ~ 460nm indicates the decay of a semiquinone at a different rate $k \sim 1500\ s^{-1}$. Measurements of $Q_A^-$ decay *via* an electrochromic absorbance change at 750nm and *via* a cytochrome assay (1) display the slower kinetics. Thus the decay of $Q_A^-$ follows the formation of another semiquinone ($Q_B^-$) suggesting the possible involvement of an intermediate state X in the electron transfer, *i.e.*

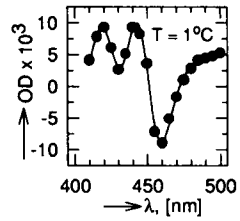


$$Q_A^-XQ_B \rightarrow Q_A^-X^+Q_B^- \rightarrow Q_AXQ_B^-$$

where electron transfer from X to $Q_B$ precedes electron transfer from $Q_A^-$ to $X^+$. (1) Debus *et al.* (1986) Biochem. 25, 2276-2287. *Supported by NSF & NIH.

**Tu-AM-C7**

DIRECT CHARGE RECOMBINATION FROM $D^+Q_AQ_B^-$ TO $DQ_AQ_B$ IN BACTERIAL REACTION CENTERS FROM *RB. SPHAEROIDES*.* ((A. Labahn, M.L. Paddock, P.H. McPherson, M.Y. Okamura and G.Feher))
Physics Dept., Univ. of California, San Diego, CA 92093

In reaction centers (RCs) from the photosynthetic bacterium *Rhodobacter sphaeroides*, the charge recombination of $D^+Q_AQ_B^-$ to $DQ_AQ_B$ proceeds indirectly via the intermediate state $D^+Q_A^-Q_B$ (1). We show from a detailed kinetic analysis that in mutant RCs in which Asp(L213) was replaced by Asn, direct recombination of $Q_B^-$ to $D^+$ ($k_{BD}$) dominates (2) below pH 8. Between pH 9 and 10 the direct and indirect pathways are about equally effective (see Figure). The recombination, $k_{BD}$, is about two orders of magnitude smaller than the recombination from $Q_A^-$ ($k_{AD}$). We attribute the large difference between $k_{BD}$ and $k_{AD}$ to a difference in the reorganization energy; this is reasonable as the environment of the $Q_B$ site is more polar than that of the $Q_A$ site. By using the classical Marcus theory of electron transfer (3), we fitted the experimental data with a reorganization energy $\lambda_{BD}$=1.23 eV, which is considerable larger than found for the $Q_A$ site in native RCs ($\lambda_{AD}$=0.64 eV) (4). The pH profile of $k_{BD}$ in native RCs was also deduced from the Marcus theory. (1) Kleinfeld et al. (1984) Biochim. Biophys. Acta 766, 126. (2) Takahashi and Wraight (1992) Biochemistry 31, 855. (3) e.g. Marcus and Sutin (1985) Biochim. Biophys. Acta 811, 265. (4) Feher et al. (1988) In: The Photosynthetic Bacterial Reaction Center (Breton, J. and Vermeglio, A., eds.), Plenum Publishing Corporation, 1988, pp.271-287. *Supported by NSF, NIH, NATO/DAAD and Deutsche Forschungsgemeinschaft

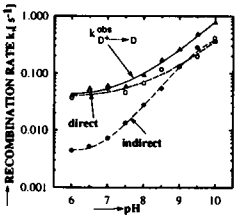


**Tu-AM-C8**

ENERGETIC INHOMOGENEITY OF $P^+H^-$ IN PHOTOSYNTHETIC REACTION CENTERS OF RB. SPHAEROIDES. ((A. Ogrodnik, W. Keupp, M. Volk, G. Aumeier and M.E. Michel-Beyerle)) Inst. für Phys. und Theor. Chemie, Technische Universität München, D85747 Garching, FRG.

Any nonuniform radical pair (RP) recombination reactions originating from energetic inhomogeneity can selectively be revealed by comparing the kinetics monitored by transient absorption and by delayed emission. While all energetically inhomogeneous RPs will contribute in the same way to the absorption signal, only the energetically high lying RPs will significantly contribute to the signal amplitude of the delayed fluorescence. Thus, the dynamics of this high energy tail of a distribution (weighed by the Boltzmann factor for repopulation of the emitting state) will determine the kinetics observed in emission, while in absorption the bulk average is reflected. We found the recombination dynamics of the RP $P^+H_A^-$ to be faster and their magnetic field dependence to exhibit a significantly broader resonance linewidth when detecting in emission than when monitoring in absorption. This points to larger values of both the singlet ($k_S$) and triplet ($k_T$) recombination rate for the high lying RP states. The observed increase of both rates with increasing energy can only be understood if superexchange coupling via $P^+B^-$ is prevailing for these recombination reactions, since its energy denominator decreases for the high lying states. The observed weak temperature dependence of the average delayed fluorescence amplitude (A) as compared to the prompt one ($A_p$) can be modelled by averaging over a Gaussian distribution of the free energy differences with a maximum at $\Delta G_0$=0.25eV and a width of $\sigma$≈0.037eV, giving $(A) = A_p \exp(-\Delta G_{app}(T)/k_BT)$ with $\Delta G_{app}(T) = \Delta G_0 - \sigma^2/2k_BT$. We attribute the deviations from monoexponential kinetics of primary charge separation and the weak electric field effects on fluorescence to this energetic inhomogeneity.

**Tu-AM-C9**

**Co-crystallization and Preliminary Structure Determination of the Photosynthetic Reaction Center and Cytochrome $c_2$ complex from *Rb. sphaeroides*** ((N. Adir, M.Y. Okamura and G. Feher))
Physics Deptartment, University of California, San Diego, La Jolla, CA 92093

The photosynthetic reaction center (RC) and cytochrome $c_2$ (cyt $c_2$) of *Rb. sphaeroides* have been co-crystallized. The co-crystals perform electron transfer from cyt $c_2$ to the photooxidized primary donor, $D^+$, of the RC. The crystals diffract x-rays to 3.5Å and belong to the tetragonal space group $P4_32_12_1$, with unit cell dimensions of $a=b$=142.7Å, $c$=254.8Å. A native x-ray diffraction data set (to 4.5Å resolution) was collected from a single crystal. A preliminary structure of the co-complex was determined in two steps: the RC was positioned by molecular replacement and the cyt $c_2$ positioned into a region of electron density not associated with the RC. The structure has been refined to an R value of 0.25. According to this solution, the cyt $c_2$ is located in the co-crystal on the periplasmic side of the M subunit of the RC (see figure), in agreement with a similar proposal by Tiede and Chang (Isr. J. Chem. 28, 183-191, (1988)). Supported by grants from NSF, NIH and USDA.

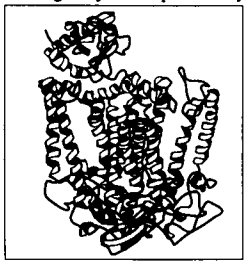

**Tu-AM-D1**

GATING AND IONIC CURRENTS FROM N-TERMINAL DELETION MUTANTS OF THE CARDIAC $CA^{2+}$ CHANNEL $\alpha_1$ SUBUNIT. ((X.Y. Wei, A. Neely, R. Olcese, E. Stefani, and L. Birnbaumer)) Dept. Molecular Physiology and Biophysics, Baylor College of Medicine, Houston, TX 77030.

We investigated the functional role of the amino terminus of the cardiac $Ca^{2+}$ channel $\alpha_1$ subunit by constructing deletion mutants. The mutants were expressed in *Xenopus* oocytes, and gating and ionic currents were recorded using the cut-open oocyte vaseline gap voltage clamp method. The maximum conductance (Gmax) for the wild type $\alpha_1$ was 1.1 μS. Deletion of 40 (ΔN40) to 120 (ΔN120) amino acids at the 153 amino acids long amino terminus resulted in dramatic increases in the amplitute of inward $Ba^{2+}$ currents, the Gmax values were 6.9 to 9.3 μS. The fitted maximum charge movement (Qmax) was 37 pC for the wild type, and from 208 to 279 pC for the mutants. The ratio of Gmax/Qmax remained unchanged. Thus, the increase in ionic currents can be explained by an increase in the number gating units (or channels) expressed in oocytes. The high levels of expression allow reliable and easy characterization of both ionic and gating currents. The currents expressed by these mutants demonstrated similar characteristics to the wild type channel. For example, the activation of the currents can be fit into a fast and a slow components; neither the rate constants nor the relative amplitude of the two components were altered by the mutants. Deletion of 145 amino acids (ΔN145), however, resulted in larger ionic currents than the wild type $\alpha_1$, without detectable gating currents. In addition, currents expressed by ΔN145 has only the fast component. It is possible that the amino acids immediately before the first predicted transmembrane segment are involved the control of channel activation.

**Tu-AM-D2**

DIFFERENTIAL CONTRIBUTION BY FOUR GLUTAMATES TO HIGH-AFFINITY $Ca^{2+}$-BINDING IN THE PORE OF A HUMAN CARDIAC L-TYPE $Ca^{2+}$ CHANNEL. ((A. Bahinski, A. Yatani, G. Mikala, S. Tang and A. Schwartz)) Dept. of Pharmacology & Cell Biophysics, University of Cincinnati, Cincinnati, OH 45267-0575

$Ca^{2+}$ channels select for divalent over monovalent cations by high-affinity binding in the permeation pathway. Recently, we have identified four highly conserved Glu (E) residues as critical in determining ion-selectivity and permeability of a human cardiac L-type $Ca^{2+}$ channel (Tang et al., 1993; Mikala et al., 1993). Single Glu to Lys (K) mutations were made in each of the pore-lining SS1-SS2 regions of the four repeats and the channels were expressed in Xenopus oocytes. Each of the mutants permeated monovalent cations, however, E1387K (repeat IV) was the only mutant which effectively permeated $Ba^{2+}$. Apparent affinity for external $Ca^{2+}$ and $Mg^{2+}$ was assessed by block of inward $Li^+$ current ($I_{Li}$) through the channels. The order of $IC_{50}$'s for $Ca^{2+}$ block of $I_{Li}$ was: E677K>E1086K>E334K>E1387K>wild-type. The order of $IC_{50}$'s for $Mg^{2+}$ block of $I_{Li}$ was: E1387K>E334K>E1086K>E677K>wild-type. The results are consistent with the concept that these four Glu residues form part of an array of high-affinity "ligands" which coordinate divalent cations within the permeation pathway of the Ca channel (Kuo, C-C. and Hess, P., 1993). In addition, the data suggest that $Glu^{1387}$ (repeat IV) may occupy a position closer to the external mouth of the pore relative to the other three Glu residues.

**Tu-AM-D3**

SINGLE MUTATIONS WITHIN THE HIGH-AFFINITY $Ca^{2+}$-BINDING REGION OF A HUMAN CARDIAC L-TYPE $Ca^{2+}$ CHANNEL ALTER SINGLE-CHANNEL CONDUCTANCE. ((A. Yatani, A. Bahinski, G. Mikala and A. Schwartz)) Dept. of Pharmacology & Cell Biophysics, University of Cincinnati, Cincinnati, OH 45267-0575

We have demonstrated that highly conserved Glu (E) residues in the pore-lining region of $Ca^{2+}$ channels are critical for high-affinity divalent cation binding and that their contributions are unequal. To test the importance of these Glu residues in ion permeation, single E-A mutations in repeats II and IV were made and single-channel currents carried by $Ba^{2+}$ and $Ca^{2+}$-block of whole-cell $I_{Li}$ were analyzed in Xenopus oocytes. Both E677A and E1387A showed higher $IC_{50}$'s (4.56 μM) for $Ca^{2+}$-block of $I_{Li}$ than wild-type (0.31 μM) and exhibited an altered unitary current amplitude (32, 21, 25 pS, for E677A, E1387A, wild-type; Fig.). The results indicate that the different effects on conductance result from an asymmetric arrangement of $Glu^{677}$ and $Glu^{1387}$ within the pore. Disruption of the outer high-affinity site ($Glu^{1387}$) results in stabilization within the inner site(s) and a decreased single-channel conductance. Destabilization of the inner site ($Glu^{677}$) results in weaker divalent-binding and an increased single-channel conductance.

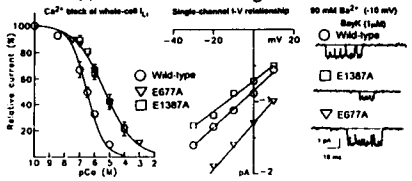


**Tu-AM-D4**

EFFECTS OF FULL OR PARTIAL REPLACEMENT OF FOUR GLUTAMATE RESIDUES ON ION PERMEATION IN THE L-TYPE $Ca^{2+}$ CHANNEL PORE. ((J.Yang, P.T. Ellinor, W.A. Sather, J-F. Zhang and R.W. Tsien)) Dept. Mol. & Cell. Physiol., Stanford Univ., Stanford, CA 94305

$Ca^{2+}$ channels select $Ca^{2+}$ by high-affinity binding to four conserved glutamate residues in the pore-lining regions of each of the four repeats in the $\alpha_1$ subunit. We have carried out a systematic series of mutational studies to characterize the contribution of each glutamate in $Ca^{2+}$ selectivity and permeation. $Ca^{2+}$ binding is assessed by examining block of inward $Li^+$ current. Replacement of all four glutamates with alanine or glutamine drastically reduced inward monovalent or divalent cation currents and abolished high-affinity $Ca^{2+}$ binding, increasing $IC_{50}$ from 1 μM in wild-type to 1.2-1.3 mM in the mutants. This supports the idea that the pore does not possess any high-affinity $Ca^{2+}$ binding site independent of the four glutamates. In each of the six possible double alanine mutants, $Ca^{2+}$ binding was attenuated by >100-fold, although substantial inward divalent cation currents remained. This suggests that the four glutamates do not form two separate sites, each with an intrinsic high-affinity for $Ca^{2+}$. Replacement of each individual glutamate with aspartate, glutamine, alanine or lysine also attenuated $Ca^{2+}$ binding to varying degrees. The pattern of changes suggests that each glutamate carboxylate participates directly in the coordination of $Ca^{2+}$, rather than acting through a purely electrostatic interaction. The mutations also altered the effectiveness of $Ba^{2+}$ ions in relieving blockade by $Cd^{2+}$ ions. This is consistent with the idea that multiple ions can interact simultaneously with the same set of glutamates. Such interactions may be essential for $Ca^{2+}$ selectivity and permeation within the $Ca^{2+}$ channel pore.

**Tu-AM-D5**

CHANGES IN SINGLE $Ca^{2+}$ CHANNEL PROPERTIES PRODUCED BY MUTATIONS IN THE L-TYPE CHANNEL PORE. ((W.A. Sather, I. Nussinovich, D.J. Gross, J. Yang & R.W. Tsien)). Dept. of Mol. Cell. Physiol., Stanford Univ., Stanford, CA 94305.

A cluster of four glutamate residues, one in each of the internal repeats, has been shown to control ion selectivity in voltage-gated L-type $Ca^{2+}$ channels (Yang et al., Nature, in press). We have carried out unitary current recordings from cell-attached patches on Xenopus oocytes to characterize the effects of amino acid substitutions at these positions on single L-type channel currents. The conductance of the wild-type $\alpha_{1C}$ expressed in Xenopus oocytes is ~25 pS in 110mM $Ba^{2+}$, as in cardiac myocytes or neurons. Channels bearing single Glu→Gln or Glu→Asp mutations exhibit decreases in $Ba^{2+}$ conductance of 25-50% relative to wild-type, with less marked changes in $Li^+$ conductance. In no case so far have we seen an increase in unitary conductance. In repeats I, III and IV, glutamine substitutions produce larger reductions in single channel $Ba^{2+}$ conductance than do homologous aspartate substitutions, consistent with the relative amplitudes of whole-cell currents carried by these mutant channels. $Cd^{2+}$ block of whole-cell $Ba^{2+}$ currents is reduced by single glutamine or aspartate mutations; at the single channel level, the reduced affinity for $Cd^{2+}$ is at least partly reflected in reduced block durations, indicating more rapid unbinding of the blocking ion from the pore. The rate of $Cd^{2+}$ unblock increases with hyperpolarization in the mutant channels, as found previously with wild-type channels in native tissue. These findings extend the results of two-microelectrode recordings, and suggest that mutations that reduce divalent cation affinity do so in large part through increases in rates of ion dissociation.

**Tu-AM-D6**

REGULATION OF THE CLONED CARDIAC CALCIUM CHANNEL BY cAMP-DEPENDENT PROTEIN KINASE. ((Edward Perez-Reyes, Weilong Yuan, Xiangyang Wei*, and Donald M. Bers)) Dept. of Physiology, Loyola University Medical Center, Maywood, IL 60153 and *Institute of Molecular Medicine and Genetics, Medical College of Georgia, Augusta, GA 30912

It is well established that cardiac L-type $Ca^{2+}$ currents are regulated by β-adrenergic agonists via a cAMP-dependent protein kinase (PKA) pathway. An underlying hypothesis is that the $Ca^{2+}$ channel itself contains the regulatory phosphorylation site. Definitive proof of this may be provided by site-directed mutagenesis of the subunit that contains this site. However, to date, regulation of the cloned cardiac $Ca^{2+}$ channel has been difficult to demonstrate. Most of these studies have used the *Xenopus laevis* oocyte system, which unfortunately contains endogenous $Ca^{2+}$ channels that are also regulated by phosphorylation. Therefore, we expressed the cardiac $\alpha_1$ and $\beta_2$ subunits in HEK 293 cells. The transfected cell expressed large dihydropyridine-sensitive currents (>5 pA/pF, 10 mM $Ba^{2+}$). In contrast to our results with cardiac ventricular myocytes, addition of forskolin failed to stimulate the currents. We hypothesized that the channel may already be phosphorylated. We tested this hypothesis using two inhibitors of PKA, rpcAMP and H-89. Both PKA inhibitors decreased the current amplitude 50-60%. Subsequent addition of forskolin (+IBMX) stimulated the currents, returning the peak current to near control values. These results provide additional evidence that the cAMP phosphorylation site resides on the channel itself.

**Tu-AM-D7**

COMPARISON OF WHOLE-CELL AND SINGLE CHANNEL PROPERTIES OF THE SKELETAL MUSCLE SLOW CALCIUM CHANNEL. ((R.T. Dirksen and K. Beam)) Department of Physiology, Colorado State University, Fort Collins, CO 80523.

Whole-cell and single calcium channel activity was measured from cultured mouse skeletal muscle in the presence of 110 mM $BaCl_2$ and Bay K 8644 (5 μM). Under these conditions the time constant of whole-cell slow calcium current ($I_{slow}$) activation becomes faster at stronger depolarizations. In addition, the conductance versus voltage (G-V) relationship is well fit by a single Boltzmann distribution with a slope of 4.8 ± 1.2 mV (n=5). The intramembrane charge movement versus voltage (Q-V) relationship is fit by a Boltzmann distribution with a slope of 13.9 ± 0.5 mV (n=10).

Cell-attached patch clamp experiments, under identical conditions, revealed a distinct $I_{slow}$ channel based on its sensitivity to dihydropyridine antagonists and similarity of its ensemble average to macroscopic $I_{slow}$. $I_{slow}$ had a single channel conductance of 14.2 ± 0.2 pS (n=10). The open probability versus voltage ($P_o$-V) relationship calculated from either the steady-state ensemble current during the pulse, or the peak ensemble tail current, was fitted by a Boltzmann distribution with a slope of 5.3 mV. Thus, the $P_o$-V relationship more closely resembles that of whole-cell channel conductance (G-V) than the shallower voltage dependence of intramembrane charge movement (Q-V). The time to first opening became progressively more rapid upon stronger depolarization. Frequency histograms of open times were typically best fit by two exponentials and were not significantly different over a wide voltage range. Additionally, at all voltages the mean open time was much briefer than the time constant of ensemble current activation. These results demonstrate that the voltage-dependence of whole-cell activation kinetics of $I_{slow}$ depend more strongly on the latency to first opening than the mean channel open time. Supported by grants AR08243 to RTD and NS24444 to KB.

**Tu-AM-D8**

EGULATION OF FAST AND SLOW GATING OF SINGLE CARDIAC L-YPE CALCIUM CHANNELS IS DIFFERENT BETWEEN THE TWO HOSPHATASE INHIBITORS OKADAIC ACID AND CALYCULIN A. (K. Wiechen and S. Herzig)) Department of Pharmacology, niversity of Kiel, 24105 Kiel, FRG

he effects of the two potent serine/threonine-protein hosphatase inhibitors okadaic acid and calyculin A on he gating behavior of single ventricular L-type calcium hannels was studied. Ten long-lasting (~1200-2400 weeps, 150 ms-steps from -100 to +20 mV, 1.6 Hz) cell-ttached recordings (70mM $Ba^{2+}$) were obtained in guinea-ig cardiac myocytes, before and after either one of the rugs, added at concentrations of ~1 μM. Both compounds nhanced the peak ensemble average current and channel vailability (fraction of sweeps containing activity). owever, while the two effects were of similar magnitude ith calyculin A (74 fA vs. 43 fA and 47 % vs. 27 %), he change in availability (38 % vs. 26%) fell short of he increase in current (100 fA vs. 44 fA) with okadaic cid. This was due to a marked increase in the fraction f sweeps with high open probability (mode 2) from 0.6% o 3.2 %. In contrast, calyculin A did not affect mode gating at all, but it hastened inactivation. Thus, the nown effects of cAMP-dependent phosphorylation are ifferently mimicked by the two phosphatase inhibitors. his suggests that separate phosphorylation sites are oupled to distinct aspects of calcium channel function.

**Tu-AM-D9**

SINGLE CHANNEL MANIFESTATION OF DUAL ACTIVATION IN CARDIAC CALCIUM CHANNEL AND ITS MODULATION BY THE BETA SUBUNIT. ((P. Baldelli, X. Wei, J. Costantin, L. Birnbaumer, E. Stefani & A. Neely, )) Dep. of Molec. Physiol. & Biophys. Baylor Col. of Med. Houston, Texas 77030.

The cardiac $Ca^{2+}$ channel $\alpha_1$ subunit ($\alpha_{1C}$) is sufficient to express voltage dependent $Ba^{2+}$ currents and coexpression of β subunit increases current density and accelerates current onset. In a previous study on macroscopic currents we proposed the existence of two modes of activation which were differentially modulated by the β subunit (Neely et al *Biophys. J. 64*: 202). Here we show two modes of channel opening at the single channel level. Patch-clamp recordings of single channel activity were obtained from *Xenopus* oocytes expressing a deletion mutant of $\alpha_{1C}$ (ΔN60, Wei et al, this meeting) in the on-cell configuration using 79 mM $Ba^{2+}$ in the presence of (-)BK 8644. Single channel activity was evoked by depolarizing steps (from -30 mV to +30 mV) from a holding potential of -50 mV. Open times and burst duration histograms were generated only from sweeps containing openings to a single level. For oocytes expressing ΔN60 alone, activity is dominated by isolated opening with a mean time of about 2 ms (at 0 mV) but near 20% of the opening had a mean open time of 10 ms. In contrast, these longer openings account for near 70% of the activity in oocytes coexpressing the β subunit. In a parallel study we show that the fraction of long openings is further increased by phosphorylation (Costantin et al, this meeting). In summary, the potentiation of macroscopic inward currents by coexpression of the β subunit can be accounted for by an increase in the fraction of channels that open with long openings and appears to correlate with the fast component of activation. (Supported by an NRSA fellowship to A. N. and grants HL37044 to L. B. and AR38970 to E. S. from NIH).

**Tu-AM-D10**

CRITICAL ROLES OF THE S3 SEGMENT AND S3-S4 LINKER OF REPEAT I IN ACTIVATION OF L-TYPE CALCIUM CHANNELS. ((J. Nakai*+, B.A. Adams*, K. Imoto+ and K.G. Beam*))*Dept. of Physiology, Colorado St. Univ., Ft. Collins CO 80523 and +Dept. of Med. Chem., Kyoto Univ., Kyoto, Japan.

Previous analysis of chimeras of the skeletal and cardiac dihydropyridine receptors (DHPRs) has revealed that repeat I is important for determining the rate of activation of L-type calcium channels. We have now made several repeat I chimeras between the skeletal and cardiac DHPRs and expressed them in dysgenic myotubes. We found that the amino acid composition of the S3 segment of repeat I (IS3) and the linker connecting IS3 to IS4 is critical for activation kinetics of the L-type channel. Mutant DHPRs which have the skeletal muscle DHPR sequence in this region activated relatively slowly with a time constant of current activation ($\tau_{act}$) > 5 ms, whereas mutants which have the cardiac sequence there activated relatively rapidly with $\tau_{act}$ < 5 ms. Comparison of the skeletal muscle and cardiac sequence in this region indicates that a total of 11 conservative and 10 non-conservative amino acid changes are sufficient to convert activation from slow to fast. The midpoint voltage for activation of L-type calcium conductance showed no consistent differences between constructs producing slow or fast activation. Thus, this region may be involved in the channel opening change that occurs only after the voltage sensor has responded to depolarization. Supported by Ministry of Education, Science and Culture, Institute of Physical and Chemical Research, Japan; and the US National Institutes of Health (NS24444).

## THEORY II

**Tu-AM-E1**

RELIABILITY OF THE ENTHALPY CHANGE DERIVED FROM VAN'T HOFF PLOTS. ((Gregorio Weber)), Department of Biochemistry, University of Illinois, 600 S. Mathews, Urbana IL 61801.

No direct method permits separation of the change in entropy of the environment (=ΔH) from the change in the entropy of the reagents (=TΔS). This is usually done by plotting ΔG/T against 1/T, and equating the slope with ΔH (van't Hoff plot). As ΔH and ΔS are both functions of the temperature:

$$d(\Delta G/T)/d(1/T) = \Delta H + [(1/T)\, d\Delta H/d(1/T) - d\Delta S/d(1/T)] \quad (1).$$

The existence of a single, characteristic ΔH depends upon cancellation of the two terms within the square brackets in (1), =ΔC, qualitatively expected as a consequence of enthalpy-entropy compensation. Estimation of ΔC requires explicit assumptions on the relations of the changes in ΔH and ΔS associated with the bond exchanges and of their temperature dependence. By the methods that I described in *J. Phys. Chem.* 97, 8108-8115, 1993, I derived the changes in ΔH and TΔS in the association of two identical protein monomers in solution to form a dimer, at a series of temperatures. Small changes in the expansivities have no significant effect on the computed ΔH and ΔS, and ΔC is almost constant with temperature, so the linearity of the plot of ΔG/T against 1/T is not disturbed. However, the enthalpies from the van't Hoff plots differ by over 50%. The worth of the van't Hoff plot depends upon $\Delta C << \Delta H$, and the credence to be given to many enthalpy values thus computed critically depends on such constraint.

**Tu-AM-E2**

THEORIES OF SOLVATION FOR BIOLOGICAL MACROMOLECULES. ((T. Ichiye, C. S. Babu, J.-K. Hyun, Y. Liu, P. D. Swartz and R. B. Yelle)) Department of Biochemistry/Biophysics, Washington State University, Pullman, WA 99164-4660.

Solvation of biological macromolecules plays a vital role in their structure and function. Three different aspects of this solvation are considered here. First, a statistical mechanical density functional theory of solvation is described which predicts the structure of water around compact globular molecules such as proteins. This type of theory can thus be used to replace explicit solvation in molecular dynamics and other computer simulations of proteins. Second, a theoretical expression in terms of an effective local dielectric constant is described which predicts the orientation of water molecules around charged molecules and which can thus be used to calculate the solvent contribution to the electrostatics of a protein. The effective local dielectric constant has been calculated for both positively and negatively charged ions from molecular dynamics simulations. Finally, molecular dynamics simulations of counterions around a globular protein are used to study the contribution of counterions to the stability and electrostatics of a protein in aqueous solution.

**Tu-AM-E3**

SOLVENT OR POLAR GROUP DYNAMICS IN ELECTRON TRANSFER REACTIONS ((V.B.P. Leite and J.N. Onuchic))
Department of Physics, University of California at San Diego, La Jolla, CA 92093.

The dynamics of solvent polarization or polar groups in proteins plays a major role in the control of electron transfer in chemical or biological systems. Recently, the thermodynamics of a simple analytical model that includes each solvent molecule (or polar group in biological proteins) independently was presented in the context of electron transfer reactions [1]. This model predicts two phases with different dynamics: (*i*) Below a critical temperature it has a glassy phase with a slow dynamics. (*ii*) Above the critical temperature it exibits a normal phase, where the linear response picture of Born-Marcus model is recovered. We will present a study on the dynamics of this model. Evidences for the glassy phase will be given. The existence of a "dynamical" phase transition depends on the value of the interactions between solvent molecules and between the solvent and the charge cavity. A phase diagram for this model will be shown. A discussion of how these different regimes may affect the rate of electron transfer will be given.

[1] J.N. Onuchic, P. Wolynes *J. Chem. Phys.* **98**,2218 (1993).

*Supported by NSF Grant # DMB-9018768 and the Department of Energy's Advanced Industrial Concepts Division. VBPL is partially supported by CNPq Brazilian agency.

**Tu-AM-E4**

Theoretical Description of Protein Hydration- A Potential of Mean Force Calculation Based On Two and Three Particle Correlation Functions.
((Angel E. Garcia, Gerhard Hummer and D. Mario Soumpasis))
Theoretical Biology and Biophysics Group, Los Alamos National Laboratory, Los Alamos, NM 87545 and Department of Molecular Biology, Max Planck Institute for Biophysical Chemistry, PO Box 2841, D-37018, Gottingen, Germany.

The local density of water around a biomolecule is constructed from calculated two point and three point correlation functions of polar and non-polar groups in water using a potential of mean force expansion. As a simple approximation, all protein atoms are classified as polar (P) (including charged) and non-polar (N). Pair and triplet correlation functions of solute and solvent (W) for all possible combinations (PW, NW, PPW, PNW, NNW) of particles are calculated by molecular dynamics simulations of dilute solutes in water. The hydration of crambin and myoglobin in solution and in the crystal environment will be described and compared with available X-ray and neutron diffraction data. The accuracy and computational efficiency of the method will be discussed.

**Tu-AM-E5**

ROLE OF ELECTROSTATICS IN PROTEIN-PROTEIN ASSOCIATION. ((Stuart P. Slagle, Richard E. Kozack, & Shankar Subramaniam)) National Center for Supercomputing Applications, Beckman Institute, Center for Biophysics and Computational Biology, and Department of Physiology & Biophysics, University of Illinois, Urbana, IL 61801

Protein–protein association is mediated to a large extent by electrostatic interactions. In this poster, we present an analysis of electrostatic interactions in two protein complexes. The electrostatic potentials and energies of interaction are obtained from the solution of the corresponding non–linear Poisson–Boltzmann equation. Using the putative model, proposed by Salemme, for the cytochrome b5/ cytochrome c complex, we have computed the electrostatic free energy of interaction for the wild–type and a series of point and double mutants. The relative electrostatic free energies correlate extremely well with the experimental free energies and thermodynamic volume change for disocciation measured by Sligar and coworkers. A similar study was also carried out for the anti–hen egg lysozyme antibody HyHel–5/HEL complex for which a high resolution structure is available. The electrostatic components of the association were delineated at the residue level in both complexes. (Supported by NIH Graduate Training Grant and by NIH grant NIGMS–GM46535)

**Tu-AM-E6**

MULTIGRID-BASED NEWTON ITERATIVE METHOD FOR SOLVING THE FULL NONLINEAR POISSON-BOLTZMANN EQUATION. ((M. Holst[1], R. E. Kozack[2], F Saied[1], and S. Subramaniam[2])) [1]Numerical Computing Group and Department of Computer Science and [2]Beckman Institute, Department of Physiology and Biophysics, National Center for Supercomputing Applications, University of Illinois, Urbana, IL 61801

A novel approach, combining multigrid techniques with damped inexact Newton iteration, is described as a means of solving the nonlinear Poisson-Boltzmann equation. The time required for solution, which is less than that for single-grid approaches in solving the corresponding linearized equation, is proportional to the number of unknowns enabling applications to large systems. The method is used to find the electrostatic field around a variety of proteins including the 1266-residue tryptophan synthase dimer. The inclusion of the full nonlinearity implies that the potential scales logarithmically with charge and thus mitigates the biological effects of highly charged groups on macromolecular surfaces. Implications for Brownian dynamics simulations of electrostatic steering are considered. (Supported in part by grants from the NIH, NSF, DOE and FMC Corporation.)

**Tu-AM-E7**

STRUCTURAL INFORMATION IN THE LOCAL ELECTRIC FIELD OF DISSOLVED DNA. ((G. Edwards, D. Hochberg, and T.W. Kephart)) Department of Physics and Astronomy, Vanderbilt University, Nashville, TN 37235.

We have developed a theoretical model of the electric potential and field for DNA in solution to investigate the persistence of structural information in the local potential or field. A Green function technique is used to account for each atom as a partial charge at its atomic coordinate. We have used partial charges from Renugopalakrishnan et al [Biopolymers 10, 1159 (1971)] for the backbone and from Pearlman and Kim [Biopolymers 24, 327 (1985)] for the bases in the structural parameters determined by Arnott and Hukins [Biochem. Biophys. Res. Commun. 47, 1504 (1972)]. In addition to the DNA macromolecule, concentric regions of condensed ions and bulk solvent are modeled as dielectric media with cylindrical symmetry. The resulting analytical expressions manifest the symmetry of the system. More specifically, the leading term is equivalent to a continuous line charge reflecting cylindrical symmetry. A subset of higher-order terms correspond to helical symmetry with a characteristic length scale of 5Å beyond the surface of DNA. Another subset of higher-order terms are due to partial charges of the bases and have a characteristic length scale of several angstroms beyond the DNA surface. These results have significance for investigations of nucleic acid-protein interactions and for experimental efforts to image biopolymers with scanning force microscopies.

**Tu-AM-E8**

COMPUTATIONAL ANALYSIS OF THE ENZYME REACTION IN MALATE DEHYDROGENASE USING A HYBRID QUANTUM/CLASSICAL METHOD
P. A. Bash, Argonne National Laboratory, Argonne, IL 60439

The enzyme reaction mechanism of Malate Dehydrogenase (MDH), which catalyzes the interconversion of malate and oxaloacetate in the citric acid cycle, is analyzed through a computer simulation methodology that combines a quantum mechanical method (MOPAC) together with molecular dynamics (CHARMM). The simulations provide a detailed depiction of the pathways, which includes the transition state structure and energetics, for the proton and hydride transfers that characterize the MDH mechanism. The results of the simulations show that the enzyme has a dramatic effect on the stabilization of the transition state and intermediates along the reaction pathway. Specifically, the enzyme stabilizes the formation of malate over oxaloacetate, in agreement with experiment, whereas, the reacting components of His-177, NAD(H), and malate/oxaloacetate arranged in a competent geometry for catalysis in the gas phase strongly favors oxaloacetate over malate. In addition to this global behavior of the enzyme solvent environment, a quantitative analysis of the role each amino acid has on the specificity of the substrates for MDH as well as the stabilization of reaction intermediates is presented.

**Tu-AM-E9**

## Lanthanide-Induced Intersystem Crossing in Model Systems - A Parametric Scheme

((*William R. Kirk* Mayo Clinic, Rochester MN, 55905))

With the synthetic compound indolylethylenediaminetetraacetic acid we investigated the binding and quenching of indole fluorescence by lanthanide ions (*J. Phys. Chem.* 92, #40, 10326, (1993)) as a potential model system of the quenching mechanisms induced by lanthanides of protein tryptophyl fluorescence. We succeeded in disentangling the contribution to quenching induced by enhanced instersystem crossing from that contributed by other mechanisms (such as dipole-dipole energy transfer) for those lanthanides which are luminescent (Tb, Sm, Dy). An unresolved question from that study was: how can one gauge the degree of quenching from enhanced intersystem crossing induced by those lanthanides which are *not* luminescent? We identify two mechanisms: 1) a direct interaction representing the sum of the spin-orbit coupling of one electron with the Coulomb field of the other, with the coupling of the magnetic moment of the latter in the orbital current of the first, and 2) the lanthanide/indole spin exchanged-orbit interaction. We apply formulae from M. Blume and R.E. Watson, *Proc. Roy. Soc. A* 270, 127 (1962), for the two-electron interactions, together with group-theoretical considerations and known lanthanide radial functions to obtain parameters for each of the lanthanides which can be combined with 3 fluorophore-dependent parameters (thus requiring data from three lanthanide complexes to specify) in order to obtain predictions for the spin-other-orbit-induced intersystem-crossing quenching rates for the other lanthanides (Pr, Nd, Ho, Er, Tm). These are compared with experiment. Other considerations may be important in other systems (those with no unpaired spins) responsible for "external heavy-atom effects".

**Tu-AM-E10**

A NEW MINIMUM PRINCIPLE FOR NONLINEAR SYSTEMS FAR FROM EQUILIBRIUM. ((J.S. Shiner* and S. Sieniutycz†)) *Physiol. Inst., Univ. Bern, Switzerland and †Dept. Chem. Eng., Warsaw Tech. Univ., Poland.

We will show that the equations of motion for a large class of discrete systems, including most, if not all, systems of biological interest, are given by the minimization of the function $P \equiv dG/dt - \partial G/\partial t + F + \Psi$ with respect to the coordinates $q_i$, the velocities $\dot{q}_i$, and the accelerations $\ddot{q}_i$ of the system. $G \equiv \sum \dot{q}_i(\partial L/\partial \dot{q}_i) - L$ is numerically equal to the Hamiltonian, but is to be considered a function of the coordinates and velocities, not of the coordinates and momenta. $L \equiv T - U$ is the Lagrangian, defined as the difference in the kinetic (co)energy $T$ and the free energy $U$. $F \equiv (1/2)\sum R_i \dot{q}_i^2$ has the form of a Rayleigh dissipation function, where the $R_i$ are generalized resistances. $\Psi \equiv (1/2)\ \sum\left[(d/dt)(\partial L/\partial \dot{q}_i) - (\partial L/\partial q_i)\right]^2 / R_i$ is the generating function, numerically equal to $F$. Since the $R_i$ as well as $L$ may be arbitrary functions of the $q_i$ and the $\dot{q}_i$, the minimum principle is of great generality. Within its scope are electrical networks, mechanical systems, both of which may display nonlinear behavior, as well as systems of chemical reactions, which are inherently nonlinear. In addition the formalism encompasses mechanochemical phenomena (muscle contraction) and electrochemical phenomena (the action potential). Examples will be given.

## BIOPHYSICAL APPROACHES TO DNA REPLICATION

**Tu-AM-SymII-1**

MOLECULAR RECOGNITION DURING DNA REPLICATION.
K. A. Johnson ,W.Kati, and K. S. Anderson. Pennsylvania State University, University Park, PA,16802; and Yale University Medical School, New Haven, CT, 06510.

DNA replication fidelity represents a difficult molecular recognition problem for DNA polymerases. These enzymes must discriminate correct from incorrectly base-paired deoxy-NTP's, as well as discriminate the correct dNTP from its ribo-NTP counterpart. We have studied the molecular recognition process for nucleotide incorporation by the DNA polymerase from phage T7 and HIV reverse transcriptase by using a well-defined synthetic primer/template oligonucleotide substrate and rapid chemical quench-flow techniques. The kinetics of incorporation of several nucleotides and nucleotide analogs were measured during a single enzyme turnover. These results, along with those determined previously for correct and incorrect incorporation by Patel and coworkers (*Biochemistry* **30**, 511-537, 1991), will be used to show how the binding energy from various substituent groups contribute to specificity of nucleotide incorporation and provide selectivity in exonuclease error correction. Recognition of mispair geometry is faciliated by a rate-limiting conformational change in the enzyme which precedes catalysis. (Supported by NIH grants GM 44613 and GM 14469).

**Tu-AM-SymII-2**

STRUCTURE AND MECHANISM OF A REPLICATIVE COMPLEX: THE DNA POLYMERASE III HOLOENZYME.
Charles McHenry, Dept. of Biochemistry, University of Colorado Health Science Center.

**Tu-AM-SymII-3**

**SUBUNIT DYNAMICS IN THE MULTIPROTEIN REPLICASE OF *E. COLI*, DNA POLYMERASE III HOLOENZYME** Mike O'Donnell, Microbiology Department and Howard Hughes Medical Institute, Cornell University Medical College, 1300 York Avenue, NY, NY 10021

The 10 subunit replicase of *E. coli*, DNA polymerase III holoenzyme (Pol III), couples hydrolysis of ATP to a tight grip on primed DNA and afterward is highly processive in synthesis without further ATP. Study of individual subunits and subassemblies of Pol III have revealed the molecular basis of its high processivity. A 5 subunit subassembly, the γ complex, functions to couple ATP hydrolysis to transfer of the β subunit from solution to primed DNA. Biophysical studies show this β subunit to be bound to the DNA by virtue of its topology, presumably by encircling the DNA like a doughnut. X-ray structure analysis showed the β dimer is indeed in the shape of a ring. The β ring slides freely along DNA and binds the polymerase subunit of Pol III. Thus the high processivity of Pol III is rooted in a β DNA sliding clamp which continually tethers the polymerase down to the template for high processivity. This picture of a polymerase with a sliding clamp riding along behind it fits with the need to synthesize long chromosomes. However, one strand of the chromosome is synthesized as a series of fragments and Pol III must be capable of hopping rapidly from one fragment to another. Study of this hopping reaction reveals a novel mechanism whereby Pol III "knows" when it has completed a DNA chain and then it rapidly separates away from its sliding clamp and reassociates with a new sliding clamp preassembled on another primed template. Study of γ complex shows it to act catalytically and is a powerful enough clamp loader to provide these β clamps at the rate needed for stoichiometric clamp consumption during replication.

**Tu-AM-SymII-4**

FUNCTIONAL COMPONENTS AND INTERACTIONS WITHIN THE BACTERIOPHAGE T4 DNA REPLICATION COMPLEX. ((P.H. von Hippel, F. Dong, E.P. Gogol, M.K. Reddy, and M.C. Young)) Institute of Molecular Biology, University of Oregon, Eugene, OR 97403.

The seven protein bacteriophage T4 DNA replication complex consists of a central polymerase that catalyzes template-directed nucleotide insertion into (and excision from) the nascent DNA, an accessory proteins subassembly that controls the stability and regulates the processivity of the overall synthesis process, a helicase-primase subassembly that opens the template DNA in front of the replication fork and primes lagging strand replication, and a single-stranded DNA binding protein that stabilizes the transiently single stranded regions of the fork and facilitates interactions within the complex. The accessory proteins subassembly consists of a DNA stimulated ATPase (the gene 44/62 proteins complex) that binds at primer-template junctions within the replication fork and catalyzes the interaction of the processivity factor of the system (the gene 45 protein trimer) with the polymerase. The helicase-primase subassembly consists of a hexamer of gene 41 protein helicase subunits that interacts with a monomer of gene 61 protein primase to form the functional primosome. Recent progress in understanding the structure, function, and interactions of these components, both alone and within the integrated T4 DNA replication complex, will be described.

**Tu-AM-F1**

## THE Na/Ca-EXCHANGER IS AN EFFECTIVE MECHANISM TO LOAD THE SARCOPLASMIC RETICULUM WITH $Ca^{2+}$ IN CARDIAC MYOCYTES

((Ana-Maria Vites and J. Andrew Wasserstrom)) Reingold ECG Center, Northwestern Univiversity Medical School, Chicago, IL-60611

The role of the Na/Ca exchanger in the heart has been primarily considered one of $Ca^{2+}$ extrusion during the relaxation of contraction. We used isolated cat ventricular myocytes to study the role of the Na/Ca exchanger as a mechanism to load the sarcoplasmic reticulum (SR) with $Ca^{2+}$. Single cell shortening and switch electrode voltage clamp techniques were used in this study. An increase in available SR $Ca^{2+}$ can be detected as a greater contraction during the subsequent beat. In the presence of nifedipine (2-20μM), we monitored cell shortening under voltage clamp conditions (T=32±1°C). A strong conditioning depolarizing step ($V_{cond}$ > +20mV, 100msec) promoted SR $Ca^{2+}$ accumulation as determined by the contractile response to a subsequent test step depolarization to -40mV from a holding potential ($V_H$) of -70mV. Increasing the duration of $V_{cond}$ increased the degree of SR $Ca^{2+}$ loading and the magnitude of the subsequent contraction. Prolonged (>1sec) $V_{cond}$ promoted spontaneous oscillatory contractions and transient currents, most likely due to SR $Ca^{2+}$ overload. In the presence of ryanodine (10μM), a step depolarization to -40mV from $V_H$= -70mV failed to produce a contraction, even when the cell was conditioned by prolonged depolarization which would have produced $Ca^{2+}$ overload in the absence of ryanodine. We conclude that the reversed Na/Ca exchanger is an effective mechanism to load $Ca^{2+}$ into the SR, and may be more effective than the L-type $Ca^{2+}$ channels. Therefore, the Na/Ca exchanger is likely to play an important role in loading of SR $Ca^{2+}$ for the subsequent beat under physiological conditions.

**Tu-AM-F2**

## Myofilament $Ca^{2+}$ Sensitivity in Intact Versus Skinned Rat Ventricular Muscle

((Wei Dong Gao, Peter H. Backx, and Eduardo Marban)) Department of Medicine, The Johns Hopkins University School of Medicine, Baltimore, MD 21205

The $Ca^{2+}$ sensitivity of the myofilaments was compared before and after skinning in the same rat trabeculae at a diastolic sarcomere length (SL) of 2.2-2.3 μm. $[Ca^{2+}]_i$ was determined using fura-2 salt. Steady-state activation was achieved by stimulating the muscle at 10 Hz after 10-20 min application of ryanodine (5 μM). The muscles were then skinned with Triton X 100 (1%) for 15-25 min and subsequently activated with solutions containing varied $[Ca^{2+}]$. The intact force-$[Ca^{2+}]$ relation was highly cooperative (Hill coefficient = 4.87 ± 0.35, n = 10) with a low $[Ca^{2+}]_i$ required for half-maximal activation ($K_{1/2}$) (0.62 ± 0.03 μM). After skinning, the Hill coefficient fell to 2.72 and the $K_{1/2}$ shifted rightwards to 2.2 μM in the presence of 1.2 mM free $Mg^{2+}$. Because of uncertainty regarding the appropriate $[Mg^{2+}]$, we measured $[Mg^{2+}]_i$ at 0.72 ± 0.06 (n = 11) with Mg-fura-2 salt. When activating solutions were modified to contain $[Mg^{2+}]$ = 0.5 mM, the force-$[Ca^{2+}]$ relation was shifted to the left ($K_{1/2}$ = 0.93 ± 0.1, n = 10) with a Hill coefficient of 3.75 ± 0.37, but the changes were not sufficient to superimpose with the intact force-$[Ca^{2+}]$ relation ($p < 0.05$ vs intact). These results indicate that, in spite of the significant effect of $Mg^{2+}$ on the force-$[Ca^{2+}]$ relation in skinned muscles, the $Ca^{2+}$ responsiveness of the myofilaments is still fundmentally altered by skinning.

**Tu-AM-F3**

## SR Ca TRANSPORT IN PERMEABILIZED MYOCYTES IS DECREASED BY INHIBITORS OF BOTH cAMP-(PKA) AND Ca-CALMODULIN-(CaM-KII) DEPENDENT PROTEIN KINASES.

((Alicia Mattiazzi, Leif Hove-Madsen and Donald M. Bers)) Loyola Univ Chicago, Maywood, IL 60153.

Phosphorylation of the SR protein, phospholamban (PLB) by PKA and CaM-KII stimulates Ca-ATPase activity and SR Ca transport, but the role of CaM-KII-dependent phosphorylation is uncertain. We studied the PKA- and CaM-KII-dependent regulation of SR Ca transport in digitonin-permeabilized rabbit ventricular myocytes. Ca uptake by the SR and free [Ca] were measured with Indo-1 and Ca-electrodes in the presence of 20 μM ruthenium red and 10 mM oxalate. Neither dibutyryl cAMP (up to 500 μM), nor the non hydrolyzable cAMP analogue sp-cAMPS (up to 275 μM) affected the $V_{max}$ or the $K_d$ for Ca uptake. However, the PKA inhibitor H-89 (20-65 μM) significantly increased $K_d$ (e.g. from 307 ± 67 to 843 ± 49 nmol Ca at 40-65 μM), without significantly affecting $V_{max}$. Both CaM-KII inhibitors, KN-62 (60 μM) and a CaM-KII inhibitory peptide (10 μM) significantly decresed $V_{max}$ (e.g. for the latter from 10.95 ± 1.72 to 7.36 ± 0.94 nmol/mg/min), without consistently changing $K_d$. The effect of H-89 on $K_d$ and of KN-62 on $V_{max}$ were prevented by a monoclonal antibody to phospholamban 2D12 (consistent with the antibody removing the inhibitory effect of PLB on the SR Ca-ATPase). Upon digitonin-permeabilization the Ca pump may be close to maximal activation, so that only inhibitory effects are apparent. We conclude that phosphorylation of PLB by endogenous CaM-KII increase the $V_{max}$ of the SR Ca-ATPase, while PKA increases the Ca affinity.

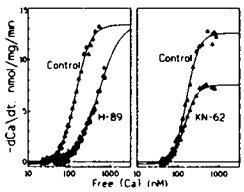


**Tu-AM-F4**

## Ca-CALMODULIN-DEPENDENT KINASE (CaMK) MODULATES $[Ca]_i$ DECLINE AND RELAXATION IN RAT CARDIAC MYOCYTES

((Rosana A. Bassani and Donald M. Bers)) Dept. of Physiology, Loyola University, Maywood IL 60153

Schouten (*J. Physiol.*, 431:427-444, 1990) proposed that prolongation of post-rest (PR) contractions was due to a deactivation of the SR Ca-pump during rest. We tested this by measuring relaxation and $[Ca]_i$ decline during twitches at steady-state (SS) stimulation (1 Hz) and after rest (PR) in isolated rat cardiac myocytes. Compared to the SS, the PR twitch after 3-5 min rest showed increased t½ for relaxation (from 104 ± 6 ms to 176 ± 7 ms) and time constant (τ) for $[Ca]_i$ decline (from 207 ± 15 ms to 391 ± 30 ms, N=6; P< 0.01). This effect appears to be related to SR Ca uptake, since we did not find changes in SR Ca content and action potential duration, or decreased ability of Na-Ca exchange to promote $[Ca]_i$ removal. The protein phosphatase inhibitor okadaic acid (5-10 μM) prevented the slowing of the PR $[Ca]_i$ decline (PR τ was decreased from 409 ± 21 ms to 282 ± 26 ms, P< 0.01) while SS τ was unchanged (from 222 ± 17 ms to 217 ± 9 ms N=7). On the other hand, inhibition of CaMK by KN-62 (10 μM) also partially suppressed the difference, but by lengthening τ for the SS twitch (SS: from 210 ± 13 ms to 311 ± 21 ms; P<0.01; PR: from 414 ± 34 ms to 407 ± 36 ms, N=5). We conclude that activation of CaMK during repetitive stimulation enhances SR Ca uptake in the rat heart, possibly via phospholamban phosphorylation.

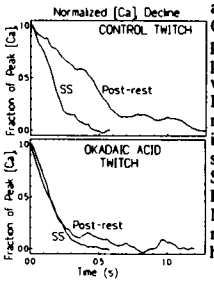


**Tu-AM-F5**

## GAIN OF CICR IN CARDIAC CELLS DEPENDS ON MEMBRANE VOLTAGE AND ON SR $Ca^{2+}$ CONTENT.

((J.R. López-López and W.G. Wier)) University of Maryland at Baltimore, MD 21021.

We measured the effect of SR $Ca^{2+}$ content on gain of $Ca^{2+}$-induced $Ca^{2+}$-release (CICR) in intact cardiac cells. Gain was defined as the ratio of peak whole-cell flux of calcium through the SR release channels ($F_{SRrel}$) to peak whole-cell flux of calcium through the L-type channels ($F_{Ica}$). $F_{SRrel}$ was computed, by methods published previously, from cytoplasmic $[Ca^{2+}]_i$ transients in single, voltage-clamped rat heart cells perfused internally with indo-1. $F_{Ica}$ was obtained from the measured $Ca^{2+}$ currents ($Cd^{2+}$-sensitive). Releasable SR $Ca^{2+}$ content was calculated using the cytoplasmic $Ca^{2+}$ transient elicited by a fast and short (5 s.) exposure of the cell to 20 mM caffeine, and the known properties of intracellular buffers in cardiac cells. We obtained the gain/voltage relationship in 7 different cells by applying 200 ms depolarizing pulses from -30mV to +80mV in 10 mV steps from a holding potential of -40 mV and at a low frequency (0.05Hz) to keep the SR loading constant. Then, SR $Ca^{2+}$ was released by application of caffeine. Total $Ca^{2+}$ released varied from about 100 μM to 250 μM (moles of SR $Ca^{2+}$ / liter accessible cell volume). In each cell (with presumed constant SR $Ca^{2+}$-content) gain was a function of clamp-pulse voltage, being high at negative potentials and decreasing towards 0 at very positive potentials (above +60 mV). When the gain obtained in diferent cells at the same membrane potential was plotted as a function of their SR $Ca^{2+}$ content, a linear correlation between gain and SR $Ca^{2+}$ content was obtained. The slopes of these lines are much greater at negative clamp pulse potentials (e.g. -20 mV) than at more positive ones. The results are discussed in terms of a 'local control' model of E-C coupling.

**Tu-AM-F6**

## REVERSE Na-Ca EXCHANGE CAN TRIGGER A PHASIC CONTRACTION IN GUINEA PIG VENTRICULAR MYOCYTES.

((O. Kohmoto, J.H.B. Bridge)) Nora Eccles Harrison CVRTI, Univ. of Utah, Salt Lake City, UT 84112

Exchanger inhibitory peptide (XIP) can inhibit Na-Ca exchange without inhibiting L-type Ca current ($I_{Ca}$). We therefore used this compound to test the hypothesis that reverse Na-Ca exchange can "trigger" contraction in guinea pig ventricular myocytes. Cells were voltage clamped with a 10mM Na pipette solution at a holding potential of -40mV and depolarized to +50mV for 0.4s at 0.25Hz. We measured cell shortening with a video motion detector. Rapid blockade of $I_{Ca}$ with 20μM nifedipine reduced cell shortening by 35% from 9.7±2.1 to 6.2±2.1μm. However, if reverse exchange was inhibited by first dialyzing the cells with 20μM XIP, blockade of $I_{Ca}$ reduced cell shortening by 60% from 6.1±0.7 to 2.5±0.3μm, suggesting that XIP inhibited a significant fraction of shortening. Cells dialyzed with solutions deficient in Na exhibited contractions that were largely dependent on $I_{Ca}$. If the sarcoplasmic reticulum (SR) was disabled with ryanodine and thapsigargin, reverse exchange could not trigger a phasic contraction. Next we measured cell shortening and action potentials in current clamped cells. Rapid application of nifedipine reduced cell shortening by 45% from 7.5±0.6 to 4.3±0.5μm. When cells were superfused with 2μM strophanthidin, blockade of $I_{Ca}$ only slightly decreased cell shortening by 15% from 10.2±1.0 to 8.7±0.9 μm. We therefore conclude that with intact SR reverse Na-Ca exchange can trigger contractions by SR Ca release in cells dialyzed with 10mM Na. In cells treated with strophanthidin which increases intracellular Na, reverse exchange appears to trigger larger contractions and presumably more SR Ca release.

**Tu-AM-F7**

**FUNCTIONAL COUPLING OF $Ca^{2+}$ CHANNELS AND RYANODINE RECEPTORS IN RAT VENTRICULAR MYOCYTES: EVIDENCE FROM THE KINETICS OF INACTIVATION OF $Ca^{2+}$ CHANNEL.** **((James S.K. Sham and Martin Morad)) Department of Medicine, The Johns Hopkins School of Medicine, Baltimore, MD 21205, and Department of Pharmacology, Georgetown University, Washington, DC 20007.**

**In a previous communication we have shown that $Ca^{2+}$ transported by $Ca^{2+}$ channel was 20 to 160 times more effective in triggering $Ca^{2+}$ release from the SR than $Ca^{2+}$ transported by $Na^+$-$Ca^{2+}$ exchanger (Science 255:850,1992), providing support for the idea that $Ca^{2+}$ channel has more direct access to the ryanodine receptors. Here we test the accessibility of $Ca^{2+}$ released from SR to sarcolemmal $Ca^{2+}$ channels by examining the effect of SR $Ca^{2+}$ release on the inactivation kinetics of $I_{Ca}$ in whole-cell clamped indo-1 dialysed (100 $\mu$M) rat ventricular myocytes. Depolarizing pulses from -60 to 0 mV activated $I_{Ca}$ and SR $Ca^{2+}$ release. $I_{Ca}$ inactivated bi-exponentially with time-constants ($\tau$) of 6.9±0.5 and 38.3±1.8 ms (n=12). Caffeine (5 mM) or ryanodine (20 $\mu$M) completely abolished $Ca^{2+}_i$ transients and significantly reduced the rate of inactivation of $I_{Ca}$ (caffeine: $\tau$=16.4±0.6 and 51.3±2.5 ms, n=10; ryanodine: $\tau$=14.9±2.3 and 53.4±4.0 ms, n=5), suggesting that $Ca^{2+}$ release from SR contributes to the inactivation of $Ca^{2+}$ channel. Caffeine had no effect on the inactivation of $I_{Ca}$ in ryanodine or $Ba^{2+}$ bathed myocytes. To determine whether global or local increase in $[Ca^{2+}]_i$ was responsible for the inactivation of $I_{Ca}$, myocytes were dialysed with 10 mM EGTA and 5 mM $Ca^{2+}$ to prevent large changes in global $[Ca^{2+}]_i$ while setting $[Ca^{2+}]_i$ at about 150 nM for adequate loading of SR. Even though $Ca^{2+}$ transients were greatly reduced in high EGTA dialysed myocytes, inactivation of $I_{Ca}$, however, remained unchanged ($\tau$=4.7±0.3 and 46.3±3.4 ms, n=5). Furthermore, caffeine still caused similar prolongation in the time-constants of inactivation (16.2±1.0 and 58.8±4.3 ms, n=5). These results, therefore, suggest that $[Ca^{2+}]$ can rise exclusively in the intracellular space around $Ca^{2+}$ channels, following activation of ryanodine receptors, when myoplasmic $[Ca^{2+}]$ was kept constant, providing further support for the "privileged pathway" between dihydropyridine and ryanodine receptors in cardiac myocytes.**

**Tu-AM-F8**

**TWO COMPONENTS OF $CA^{2+}$-ACTIVATED $CL^-$ CURRENT IN SINGLE PURKINJE CELLS FROM RABBIT HEART.**

((Zoltan Papp, Karin R. Sipido, Geert Callewaert, and Edward Carmeliet)). Laboratory of Physiology, University of Leuven, Belgium

The time course of $I_{ClCa}$ observed during depolarizing steps in single cells, is much shorter than the time course of the $[Ca^{2+}]_i$ transient (Sipido et al., 1993). However, slow $Ca^{2+}$-activated $Cl^-$ currents have been observed during $[Ca^{2+}]_i$ oscillations in rabbit Purkinje fibers (Han & Ferrier, 1992). We therefore further examined $I_{ClCa}$ during large $[Ca^{2+}]_i$ transients obtained by caffeine-induced $Ca^{2+}$ release from the sarcoplasmic reticulum, at steady membrane potentials.

Enzymatically isolated single Purkinje cells from rabbit heart were studied under whole cell voltage clamp, with $K_5$fura-2 as a $[Ca^{2+}]_i$ indicator (22°C). Na/Ca exchange and $K^+$ currents were eliminated.

Caffeine (10mM) was briefly applied at different holding potentials (-80mV in figure). During these $[Ca^{2+}]_i$ transients, two kinetically distinct components of membrane current were observed. The first component appeared during the rising phase of $[Ca^{2+}]_i$, and declined before peak $[Ca^{2+}]_i$. This current was seen in nearly all cells (n=64). The second current component was slower and followed more closely the time course of $[Ca^{2+}]_i$. It was seen in 32 out of 64 cells. $E_{rev}$ of both components was the same and shifted in the expected direction during $Cl^-$ substitutions, indicating they were both $Ca^{2+}$-activated $Cl^-$ currents.

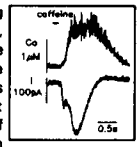


The early component has the same characteristics as $I_{ClCa}$ previously described during depolarizing steps. The second component may be related to $Ca^{2+}$ overload, as it was seen most frequently when resting $[Ca^{2+}]_i$ was elevated, and during spontaneous oscillations.

**Tu-AM-F9**

**PRIMARY OSCILLATIONS OF ATP DRIVEN BY GLYCOLYSIS IN HEART CELLS: IMPLICATIONS FOR ARRHYTHMOGENESIS AND CONTRACTILE DYSFUNCTION** ((B. Ramza, B. O'Rourke, E. Marban)) Johns Hopkins University, Baltimore, MD 21205

Biological oscillators play an important role in the regulation of insulin release, neuronal bursting and cardiac pacemaking. While oscillations in glycolysis have been extensively characterized in tissue extracts, there have been few demonstrations of this phenomenon in intact cells. We now describe an intrinsic biological oscillator with similar properties linking energy metabolism with ion channel function in single guinea-pig cardiomyocytes. Isolated myocytes (n=44) were initially bathed in a substrate-free tyrode's solution and voltage-clamped using patch pipettes filled with a high $[K^+]$ solution and moderate concentrations of ATP (0.2-5 mM). Immediately upon gaining intracellular access, 15 cells (34%) spontaneously developed large cyclical increases (5-10 nA) in a glibenclamide-sensitive current with a period of 1-2 minutes and a reversal potential near $E_K$, implicating ATP-sensitive $K^+$ channels ($I_{K,ATP}$) in the response. Simultaneous measurements of cytosolic $Ca^{2+}$ showed that the amplitude of the depolarization-evoked transient was suppressed during the peaks of these oscillations. The addition of 10 mM glucose to the bath suppressed the oscillations in current and $Ca^{2+}$ transient amplitude. To determine if the intrinsic oscillator was influenced by purine nucleotide levels, we induced sudden increases in intracellular ATP or ADP by flash photolysis. Spontaneous oscillations of $I_{K,ATP}$ were observed in half of the cells containing caged ATP before photolysis. Interestingly, oscillations could be induced (after a short lag period) in myocytes that were not oscillating prior to photolytic release of ATP. Photolysis of caged ADP also initiated oscillations with minimal delay, providing evidence that allosteric control of phosphofructokinase may be involved. Experiments showing similar oscillations in action potential duration in current-clamped myocytes suggest that the oscillator may be a factor in the pathological changes in electrical excitation as well as contractile dysfunction during periods of metabolic stress.

**Tu-AM-F10**

**IS THE BAY K 8644 INDUCED LOSS OF SR Ca DURING REST IN CARDIAC MUSCLE DUE TO A SMALL Ca INFLUX AT REST?**

((E. McCall & D.M. Bers)) Physiology, Loyola Univ., Maywood, IL 60153.

The dihydropyridine receptor (DHPR) agonist of L-type Ca channels, Bay K 8644 (BAY), accelerates rest decay of contractions and SR Ca content in dog and ferret ventricular muscle. This could be due to 1) a physical effect of the DHPR on the ryanodine receptor (RyR) or 2) a small, undetectable "window" $I_{Ca}$ during rest, causing more rapid SR depletion via Ca-induced Ca-release. We tested the latter possibility using post-rest twitches and caffeine-induced contractures (CafC) in isolated ferret myocytes at 37°C. In control solution $[Ca]_o$ was 3 mM and was reduced to 1 mM in BAY (0.1 $\mu$M) such that steady state twitches were of similar amplitude (5.7±0.5 $\mu$m *vs* 6.2±0.6 $\mu$m in BAY,n=18). BAY accelerated rest decay of twitches and CafC in control solution as expected (Fig). Even when Ca influx was completely prevented during rest by 0Ca/0Na (+ 1 mM EGTA) solution, BAY still accelerated rest decay (Fig). We conclude that Ca influx is not required for this effect of BAY and our results would be consistent with a relatively direct effect of the DHPR on the RyR.

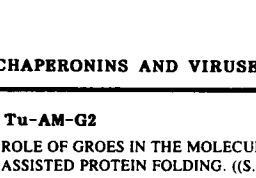


As reported by Bassani *et al.* (*J Physiol*, In Press) rest decay in ferret myocytes is not inhibited by 0Ca/0Na. This contrasts with rabbit, guinea-pig and rat, where 0Ca/0Na prevents rest decay. This suggests a less dominant role of Na/Ca exchange in Ca efflux in ferret myocytes. (supported in part by a British-American Research Fellowship from American Heart Association and the British Heart Foundation).

## FOLDING AND SELF-ASSEMBLY II: CHAPERONINS AND VIRUSES

**Tu-AM-G1**

PROGRESS ON THE CRYSTAL STRUCTURE DETERMINATION OF THE GRO-ES CHAPERONIN PROTEIN FROM *E. COLI*. ((John F. Hunt#, Arthur J. Weaver, Sam Landry†, Lila Gierasch†, and Johann Deisenhofer#)) Howard Hughes Medical Institute, (†) Department of Pharmacology, and (#) Department of Biochemistry, University of Texas Southwestern Medical Center at Dallas.

It has become apparent that the folding of some nascent proteins in living cells is controlled and possibly even catalyzed by other proteins, referred to as "chaperonins". One of the most thoroughly studied chaperonins is the groEL / groES complex from *E. coli*. We have undertaken a crystal structure determination of the groES protein in order to help elucidate the role of groES in protein-assisted protein folding. As of the time of submission of this abstract, we have collected diffraction data to 2.7Å resolution from native crystals at 130°K. We have also identified three heavy metal derivatives using Harker sections and vector verification procedures. We are optimistic about rapid progress in the structure determination; however, non-isomorphism in the low temperature data from different native groES crystals could slow down solution of the phase problem using multiple isomorphous replacement. The current status of this project will be reported.

**Tu-AM-G2**

ROLE OF GROES IN THE MOLECULAR MECHANISM OF CHAPERONIN-ASSISTED PROTEIN FOLDING. ((S.J. Landry and N.K. Steede)) Dept. Biochemistry, Tulane University School of Medicine, New Orleans, LA 70115 (Spon. by S. Landry)

The 57 kDa *Escherichia coli* chaperonin GroEL and the 10 kDa co-chaperonin GroES are encoded on the same stress-induced cistron, and both proteins are essential for growth at all temperatures. GroEL has ATPase activity, and ATP induces dissociation and concomitant folding of protein substrates. ATP binding and hydrolysis are more cooperative in the presence of GroES, and in vitro folding of some proteins is only accomplished in the presence of GroES. In the presence of ATP, the GroES 7-mer binds to one end of the GroEL 14-mer which aligns the 7-fold axes of the molecules and could allow each GroES subunit to engage a GroEL subunit. Since the GroEL/GroES complex contains stably bound ADP, binding of GroES could stabilize the nucleotide-bound conformer of GroEL or contribute directly to formation of the nucleotide binding site. The latter possibility is suggested by similarity of a functionally important GroES sequence to sequences in nucleotide-binding proteins *E. coli* FtsA and trypanosomal phosphoglycerate kinase (PGK). Previous work shows that the putative nucleotide-binding region lies within a mobile loop of GroES which becomes immobilized in the complex with GroEL; a synthetic peptide corresponding to the loop binds to GroEL in a turn-containing conformation; and mutations resulting in partially defective GroES cluster in the mobile loop [Landry, Zeilstra-Ryalls, Fayet, Georgopoulos and Gierasch, *Nature* **364**, 255-258]. Here, we show that one of these GroES mutants fails to form a complex with GroEL, possibly because the mutation disrupts contacts between the mobile loop and GroEL and/or ATP. Molecular modeling reveals that the conformation adopted by the synthetic mobile loop peptide in association with GroEL is compatible with the corresponding sequences in crystal structures of hsc70 (an FtsA homolog) and yeast PGK. GroES stabilization of GroEL-bound ADP may provide a mechanism that ensures all GroEL subunits dissociate substrate protein simultaneously.

**Tu-AM-G3**

SPONTANEOUS AND CHAPERONIN-ASSISTED REFOLDING OF RABBIT MUSCLE GLYCERALDEHYDE-3-PHOSPHATE DEHYDROGENASE

((K.C. Wisser and A. Gafni)) Department of Biological Chemistry and Institute of Gerontology, University of Michigan, Ann Arbor, MI 48109-2007

Spontaneous refolding of glyceraldehyde-3-phosphate dehydrogenase (GAPDH), denatured by guanidine: HCl was initiated by dilution of the denaturant and monitored through the recovery of enzymatic activity. The reactivation at 32°C proceeded with a half-life of ca 10 minutes and reached a limiting value of about 25% within one hour. In presence of 4 moles GroEL per mole of GAPDH tetramer, and Mg:ATP, the reactivation showed similar kinetics; however, the yield increased to ca 40%. Addition of the co-chaperonin, GroES, to the above experiment increased the reactivation yield further, to 60%, again with no significant change in the rate of refolding. When ATP was omitted from the reactivation mixture the GroEL (or GroELS)-assisted reactivation was completely arrested but could be triggered by ATP addition. When GAPDH was similarly refolded but in presence of only 2 moles GroEL per enzyme tetramer the rate and yield of reactivation in presence of Mg:ATP were practically identical to those obtained with 4 moles chaperonin. Addition of GroES, however, failed to induce any increase in reactivation yield in this case. When ATP was omitted the reactivation was strongly, but not completely, arrested, and proceeded at a rate about 15 times slower than that in presence of ATP (or that of spontaneous refolding). These results show that GroEL is capable of tightly binding at least two subunits of GAPDH and that ATP induces a rapid release of bound enzyme in a form that more effectively assembles to the active tetramer than during spontaneous refolding. GroES enhances the yield of reactivation only when one GAPDH subunit is bound per GroEL molecule. It is possible that binding of a second subunit of the refolding enzyme to the chaperonin blocks the binding of the co-chaperonin. Supported by NIA Grant AG097GI and ONR Contract N00014-91-J-1938.

**Tu-AM-G4**

FOLDING AND STABILITY OF WILD TYPE AND TEMPERATURE SENSITIVE MUTANT FORMS OF THE PHAGE P22 COAT PROTEIN

((Maria Luisa Galisteo, Carl L. Gordon, Carolyn M. Teschke and Jonathan King)) Dept of Biology, M.I.T., Cambridge, MA 02139

The gene 5 major coat subunit of P22 is synthesized as a monomer and subsequently polymerizes to form T=7 icosahedral shells. Temperature sensitive folding (TSF) mutations have been characterized at many sites in the 47kd coat protein [Gordon, C.L. & King, J. (1993) *J. Biol. Chem.* **268**, 9358-9368]. These identify amino acid sites needed for the newly synthesized chain to reach its assembly-competent subunit conformation within the cell at higher temperatures. Soluble precursor subunits carrying four such substitutions (A108V; T294I; F353L; W48Q) have been purified and analyzed by differential scanning calorimetry. The melting temperatures of subunits carrying the tsf substitutions did not differ significantly from the melting temperature of the wild type (40°C). These results indicate that the substitutions act by destabilizing an intracellular kinetic folding intermediate at the junction between aggregation and folding, rather than the folded monomer. Coat subunits can be efficiently refolded in vitro [Teschke, C.M. & King, J. (1993) *Biochem.* **32**, 10839-10847]. The kinetic refolding of the mutant proteins is currently being compared with the in vivo folding pathway.

**Tu-AM-G5**

THE EFFECT OF PRESSURE ON BACTERIOPHAGE P22 COAT PROTEIN, STUDIES WITH WILD TYPE AND MUTANT PROTEINS.

((P.E. Prevelige, J. Silva)) Boston Biomedical Research Institute, Boston MA. and Universidade Federal do Rio de Janeiro, Rio de Janeiro Brazil

Bacteriophage P22 is a well studied double stranded DNA containing bacteriophage. Capsid assembly proceeds through a series of metastable states in which the conformation of the protein differs. The mechanism by which the flexibility necessary for assembly is built into the protein subunit is of fundamental interest. A series of single point mutations in the coat protein exist. These proteins display altered folding and assembly properties. The pressure stability of wild type bacteriophage P22 coat protein in both monomeric and polymeric forms under hydrostatic pressure was examined using light scattering, fluorescence emission, polarization, and lifetime methodology. The monomeric protein is very unstable toward pressure and undergoes significant structural changes at pressures as low as 0.5 kbar. These structural changes ultimately lead to denaturation of the subunit. Comparison of the protein denatured by pressure to that in guanidine hydrochloride suggests that pressure results in partial unfolding, perhaps by a domain mechanism. Fluorescence lifetime measurements indicate that at atmospheric pressure the local environments of the tryptophans are remarkably similar, suggesting they may be clustered.

In contrast to the monomeric protein subunit, the protein when polymerized into procapsid shells is very stable to applied pressure and does not dissociate with pressure up to 2.5 kbar. However, under applied pressure the procapsid shells are cold labile, suggesting they are entropically stabilized. The significance of these results in terms of virus assembly are discussed.

**Tu-AM-G6**

USE OF BIS-ANS TO INHIBIT VIRAL CAPSID ASSEMBLY.

((P.E. Prevelige, C.M. Teschke J. King)) Boston Biomedical Research Institute, Boston MA. (PEP) and Dept of Biology, MIT, Cambridge MA. (CMT, and JK)

The precursor shells of dsDNA bacteriophages are assembled by the polymerization of competent states of coat and scaffolding subunits. The fluorescent dye 1,1'-bi(4-anilino)naphthalene-5,5'-disulfonic acid (bisANS) binds to both the coat and scaffolding proteins from the *Salmonella typhimurium* bacteriophage P22. It displays little affinity for the polymerized forms of the proteins. The subunits with bound bisANS are incapable of assembling into procapsids. The binding constants of bisANS for both coat and scaffolding protein monomers have been measured and are 5 and 6 mM respectively. Binding of bisANS to coat protein has little effect on the conformation as determined by circular dichroism and susceptibility to proteolysis. Binding of bisANS to scaffolding protein induces a change in the secondary structure consistent with a loss of a-helix, and an altered susceptibility to proteolysis. The bisANS is probably binding at sites responsible for intersubunit interactions and thereby inhibiting capsid assembly. Localization of the bisANS binding site will provide molecular information about the intersubunit contacts required for assembly. Photo-exposure of coat protein with bisANS bound results in the formation of a covalent adduct This modification does not appear to result in changes in protein conformation. Attempts to identify the covalent adduct by HPLC and amino acid sequencing of tryptic peptides are underway.

**Tu-AM-G7**

THREE-DIMENSIONAL STRUCTURE OF THE ROTAVIRUS HEMAGGLUTININ VP4 AT 26Å RESOLUTION BY CRYO-EM AND DIFFERENCE MAP ANALYSIS.

*((Mark Yeager*, John A. Berriman†, Timothy S. Baker#, and A. Richard Bellamy**))*
**Scripps Clinic and Research Foundation, Dept. of Cell Biology, La Jolla, CA, USA.*
*†MRC Laboratory of Molecular Biology, Hills Road, Cambridge, U.K.*
*#Dept. of Biological Sciences, Purdue University, West Lafayette, IN*
***Dept. of Cellular and Molecular Biology, U. of Auckland, Auckland, N.Z.*

Rotavirus is a major cause of human infant morbidity and mortality by causing severe gastroenteritis. Infection is mediated by the VP4 hemagglutinin spike which binds to cell surface receptors. We previously reported the three-dimensional structure of VP4 at 35Å resolution [*Biophys J.* 61: A7 (1992)], and the analysis has now been extended to 26Å resolution. Native and spikeless virions were mixed prior to cryo-preservation so that both structures could be determined from the same micrograph, thereby minimizing systematic errors. This mixing strategy was crucial for difference map analysis since VP4 only accounts for ~1% of the virion mass. The VP4 spike is multi-domained and has a radial length of ~200Å with ~110Å projecting from the surface of the virus. Interactions between VP4 and cell surface receptors are facilitated by the uniform distribution of the VP4 heads at maximum radius, as well as the bi-lobed head, which allows multi-site interactions. The bi-lobed head is attached to a square-shaped body formed by two rods that have a slight left-handed helical twist. These rods merge with an angled rod-like domain connected to a globular base ~85Å in diameter. The anchoring base displays pseudo-six-fold symmetry. This surprising finding may represent a novel folding motif in which a single polypeptide of VP4 contributes similar but non-equivalent domains to form the arms of the hexameric base. The VP4 spike penetrates the virion surface ~90Å and interacts with both outer (VP7) and inner (VP6) capsid proteins. Extensive VP4/VP7 and VP4/VP6 interactions imply a scaffolding function in which VP4 may participate in maintaining precise geometric register between the inner and outer capsids. The analysis also has implications for rotavirus morphogenesis. We hypothesize that VP4/VP6 interactions may allow initial binding of VP4 to immature inner capsid particles in the viroplasm, which are known to then bind to NS28 in the membrane of the endoplasmic reticulum and then bud through the membrane to acquire the VP7 outer capsid layer.

**Tu-AM-G8**

3-D STRUCTURAL STUDIES ON BACULOVIRUS-EXPRESSED ROTAVIRUS SUB-ASSEMBLIES.

((R. Rothnagel, Q-Y. Zeng*, M.K.Estes*, W. Chiu and B.V.V. Prasad)).
Department of Biochemistry, *Division of Molecular Virology, Baylor College of Medicine, Houston, TX 77030.

Rotavirus is the major cause of endemic, severe diarrhea in infants and children. It contains 11 segments of double-stranded RNA, each of which encoding at least one protein. The genes that code for the six structural proteins, VP1, VP2, VP3, VP4, VP6, VP7, and also the five non-structural proteins, NSP1-5, have been cloned and expressed. It has been shown that the co-expression of specific structural proteins result in the spontaneous formation of virus-like particles or other functional complexes. We have determined 3-D structures of VP2, VP1/2/3/6, VP2/6 particles using electron cryomicroscopy and computer image analysis. From our earlier studies, we had proposed that rotavirus is a triple-shelled virus and VP2 forms the inner most shell. Our present structural studies confirm this proposal. Baculovirus-expressed VP2 protein forms shells of diameter 520 Å. The thickness of the protein shell is about 35 Å. Comparison of the VP2 structure with the VP2/6 structure revealed that the VP6 interacts extensively with VP2. The surface morphology of the VP2/6 particles is identical to the native single-shelled particle. The structure of the VP6 molecule appears to have three domains: the globular head domain, a stem domain, and lower tail domain which forms the interface with VP2. The trimers are formed mainly through the interactions between the head domains. The inter-capsomeric interactions are mainly through the tail domains across the 2-fold axes. Our studies show that the channels in the VP6 shell terminate at the surface of the VP2 shell. The VP2 shell has small pores, around the 5-fold and icosahedral 3-fold axes. The pores around the icosahedral 3-fold axes are not in register with, but are connected to, the type III channels of the VP6 shell. In the VP1/2/3/6 structure, we see significant mass density inside the VP2 shell which can be attributed to VP1 and VP3. We acknowledge support from NIH grants and W.M. Keck Foundation.

**Tu-AM-G9**

SUBUNIT STRUCTURES IN CAPSOMERES OF HERPES SIMPLEX VIRUS CAPSID REVEALED BY 400KV SPOT-SCAN ELECTRON CRYOMICROSCOPY. ((Z.H. Zhou, J. Jakana, B.V.V. Prasad, F.J. Rixon[&] and W. Chiu)) Department of Biochemistry, Baylor College of Medicine, Houston, TX 77030; [&]MRC Virology Unit, Institute of Virology, Glasgow, Scotland

The A-capsid of herpes simplex virus type 1 (HSV1) is a T=16 icosahedral particle of 1250 Å in diameter with 4 different structural proteins. We have recorded spot-scan images of ice-embedded HSV1 capsids in a 400kV electron cryomicroscope. Modification of the software has been made to allow a 3-dimensional reconstruction to ~20 Å resolution from 200 capsid particles. An asymmetric unit contains one hexon, three types of pentons and six types of triplexes. The penton subunit has 3 domains: a diamond-shaped upper domain, a stem-like central domain and a slender lower domain. These domain features are also seen in all the hexon subunits in addition to a horn-shaped mass density at the upper domain. This confirmed our previous suggestion of the penton and hexon being made up of VP5 and the proposal of hexon also containing VP26 (A. Steven, unpublished). The lower domain among the various quasi-equivalent hexon subunits show significant conformational variability. Each of the 6 quasi-equivalent triplexes contains three dissimilar legs and an upper domain with a variable number of arms in contact with with the neighboring capsomeric subunits. The structural variability among the triplexes and also among the lower domains of the capsomeric subunits may play an important role in the assembly of herpes capsid.

We acknowledge support of W. M. Keck Foundation and NCRR/NIH.

**Tu-AM-G10**

**STRUCTURAL POLYMORPHISM OF THE HIV-MN V3 LOOP**

**P. Catasti[1,2], E. M. Bradbury[1], and G. Gupta[2]**
**[1]Life Sciences Division & [2]T-10, LANL, Los Alamos, NM**

We have investigated by NMR spectroscopy the three-dimensional folding of the HIV-MN V3-loop. MN V3 loop is a cyclic peptide stabilized by a disulfide bridge between two cystines located at positions 1 and 35. The structural studies were performed in aqueous and in mixed (water/TFE) solvents. NMR studies on the control linear peptide showed that only the central principal neutralizing determinant sequence adopted a protruding loop with a rather flexible GPGR-turn and the N- and C- terminal segments were floppy. The analyses of NMR data of the cyclic MN V3 loop in aqueous solution resulted in 200 pairwise NOESY cross-peaks corresponding to short and medium range interactions and 27 dihedral angle constraints which indicated the following effects of the cyclization: (1) induction of an N-terminal loop containing residues 1-9, (2) stabilization of the GPGR-turn, and (3) formation of a few turns in the peptide segment containing residues 25-33. The cyclic MN V3 loop in a mixed (water/TFE) solvent revealed further induction of structure in that the C-terminal residues 23-33 adopted an α-helix as indicated by monitoring the upfield αH resonance shift and by comparing the relative intensities of sequential NH-NH vs NH-αH NOESY cross-peaks. Thus, the NMR studies showed that the MN V3 loop does indeed have structure in water which can undergo polymorphic transitions in solvents of differing polarity. These results also indicate that vaccine attempts using linear peptide would be less effective than cyclic peptides in inducing humoral immunity to the conserved structural features. In this case, the use of a water/TFE mixture helps to unmask the intrinsic secondary structural propensities of the V3 loop residues. The elucidation of these higher ordered structures of the V3 loop as detected in water/TFE mixtures may be biologically relevant.

## VOLTAGE GATING IN CHANNELS

**Tu-AM-H1**

**VOLTAGE-DEPENDENCE OF SODIUM CHANNEL ACTIVATION IS ALTERED BY SUBSTITUTIONS OF S4 POSITIVE CHARGES IN DOMAINS III AND IV.** ((K.J. Kontis, A. Rounaghi and A.L. Goldin)) Department of Microbiology and Molecular Genetics, University of California, Irvine, CA 92717-4025.

The sodium channel α subunit is composed of four homologous domains with 50-70% sequence identity. Each domain is thought to consist of 6-8 membrane-spanning segments. The fourth segment, termed S4, has a repeated motif consisting of a positively charged amino acid followed by two hydrophobic residues. This structure has been proposed to be the voltage sensor of the channel. Stühmer et al. [Nature (1989) 339:597-603] provided convincing evidence that this hypothesis is correct, showing that replacement of specific positive charges in two of the S4 segments of the rat brain II channel alters the voltage dependence and gating valence. However, those studies only addressed domains I and II, and used a sodium channel with fast inactivation, which can prevent accurate measurements of peak currents. We wanted to assess the role of S4 positive charges in determining activation gating of the sodium channel in the absence of inactivation. We have used site directed mutagenesis to make charge conserving and neutralizing substitutions of the second and fourth S4 positive charges in all four domains of the rat brain IIA sodium channel. The substitutions were made in a sodium channel mutant that lacks fast inactivation. Sodium currents were elicited from *Xenopus* oocytes that were injected with in vitro transcribed RNA, and the data were analyzed to determine activation gating parameters. Neutralization of positive charges in IIIS4 and IVS4 resulted in negative shifts in the voltage-dependence of activation. In one case, a charge conserving substitution caused both a negative shift in voltage-dependence and a slight decrease in the apparent gating valence. These results indicate that domains III and IV behave in a way consistent with being parts of the voltage sensor of the channel.

**Tu-AM-H2**

TWO REGIONS OF THE CYCLIC NUCLEOTIDE-GATED CHANNELS DETERMINE AGONIST SELECTIVITY ((Evan Goulding, Gareth Tibbs, Steve Siegelbaum)) Center for Neurobiology and Behavior, Columbia University, New York, New York10032

Sensory transduction in olfactory receptor neurons and photoreceptors involves a class of ion channels, the cyclic nucleotide gated (CNG) channels, which open in response to the binding of intracellular cAMP and/or cGMP. The olfactory channel is gated equally well by cGMP and cAMP with K1/2 values (50uM) and maximal currents for cGMP and cAMP being equal. The retinal channel is selective for cGMP with a K1/2 which is 40-fold lower for cGMP (50uM) than for cAMP (2000uM) and a maximal current which is 50-fold greater for cGMP than for cAMP. Since the olfactory and retinal CNG channels exhibit distinct ligand selectivity, we have made a number of chimeras between the two channels and expressed these chimeras in *Xenopus* oocytes to determine which regions of the channels control ligand binding and gating. We focused on a carboxy terminal region of the channels that exhibits amino acid homology with the cyclic nucleotide binding domains of the catabolite activating protein and cGMP and cAMP kinases. When this region of the retinal channel is replaced by the corresponding region of the olfactory channel, the chimera has K1/2 values which are similar for cGMP and cAMP like the olfactory channel. Conversely, when this region of the olfactory channel is replaced by the corresponding region in the retinal channel, the chimera has a K1/2 for cGMP which is more than 50-fold lower than for cAMP like the retinal channel. While the relative K1/2 values of the CNG channels are determined by this cyclic nucleotide-binding domain, the relative efficacies of cGMP and cAMP are determined by a portion of the amino terminus of the channel and by the adjacent transmembrane domains.

**Tu-AM-H3**

EVIDENCE FOR A FUNCTIONAL SLIDING MOTION OF A ß-STRAND DURING VOLTAGE-GATING OF THE VDAC CHANNEL. ((M. Zizi, E. Blachly-Dyson*, M. Forte*, M. Colombini)) Dept. Zoology, UMCP, College Park, MD 20742. *OHSU, Portland, OR 97201 (Spon. by L.M. Amende)

The mitochondrial outer membrane channel VDAC forms a large aqueous pore. Experimental results indicate that one 30 kDa polypeptide form one channel whose transmembrane region consists of 1 $\alpha$ helix and 12 $\beta$ strands. Yeast VDAC reconstituted in asolectin:cholesterol membranes displays two voltage-gating processes, at negative and positive potentials, whose voltage-dependence parameters are virtually identical ($n=25\pm1$ vs $n=25\pm1$ with 58$\mu$g/ml dextran sulfate known to amplify the voltage dependence 10 fold). Thus the number of effective charges on each sensor is the same ($\approx 2.5$). One point mutation in a ß-strand, E152K, close to the mouth of the pore, affects the gating charge in an asymmetrical way ($n=36\pm1$ vs $n=26\pm1$) indicating that the charge crosses the electric field during only one gating process. A second mutation, E145K, located at the other end of the same ß-strand and close to the opposite mouth of the channel, displays the same asymmetrical effect ($n=24\pm1$ vs $n=39\pm1$). Once more this would be compatible with the charge moving through the field in one direction only. If this ß-strand were to slide relatively to the plane of the membrane, a double-mutant should have an additive effect. As expected, the double mutant E145K/E152K shows increased voltage dependence for both gating processes ($n=37\pm1$ vs $n=39\pm1$). The fact that the free energy differences between the two gating processes (nFVo) of the double-mutant gating (2 kJ/mole) is equal to the sum for the two single-mutants (2 kJ/mole for E152K and $\approx 0$ kJ/mole for E145K) argues that the two mutations are independent of each other and do not interact significantly. Thus, in addition to the previously reported large-scale motion of portions of the channel wall out of the pore region, one of the remaining $\beta$ strands seems to slide toward one or the other surface depending on the sign of the applied voltage. This motion may have important implication on the structure and accessibility of the surface domains.

**Tu-AM-H4**

**CARDIAC GATING CHARGE MOVEMENT: FAST AND SLOW COMPONENTS OF $Q_{OFF}$.** **((I.R. Josephson and Y. Cui))** Physiology and Biophysics, University of Cincinnati, Cincinnati, OH 45267-0576.

Nonlinear charge movement during membrane depolarization ($Q_{ON}$) of cardiac ventricular myocytes has been separated (by kinetic and steady-state criteria) into constituent components associated with the activation gating of Na channels and Ca channels. In contrast, the nature and time course of the OFF charge movement following membrane repolarization has not been as clearly established. To investigate this point the nonlinear ON and OFF charge movements have been studied using small-diameter, embryonic ventricular myocytes that can be rapidly and uniformly voltage clamped. Brief (5.4 msec) depolarizing steps were employed to produce Na channel inactivation, with little Ca channel inactivation. Following the return of the membrane potential to -100 mV the OFF charge movement displayed two kinetic components. Double exponential fits to $Q_{OFF}$ yielded time constants of a few tenths of a msec for the fast, large-amplitude component, and several msecs for the slower, small-amplitude component. The time course and voltage dependence for the slowly-decaying component suggests that it may be linked to the recovery of Na channels from inactivation, as has been demonstrated for nerve axon. Thus, cardiac $Q_{OFF}$ (after a brief depolarization) is predominantly composed of the fast return (deactivation) of non-inactivated Ca channel charge, followed by the slower return of inactivated Na channel charge. Supported by NIH and AHA grants to IRJ.

**Tu-AM-H5**

GATING CURRENTS FROM A SINGLE POTASSIUM CHANNEL MOLECULE.
((Yuval H. Mika and Yoram Palti)) Rappaport Family Inst., B. Rappaport Faculty of Med. & B. kats Cell Biophys. Minerva Center, Technion, Haifa, Israel.

To date gating currents, which reflect the channel molecule conformational changes, were measured only from an ensemble of numerous channels. This study presents, for the first time, measurements of gating currents from a single potassium channel molecule. Single channel pre-open gating current, measured by averaging ~8000 events aligned to the channel opening time, consists of 2 components: 1. A relatively constant current averaging 2fA. 2. Short current transients, time locked to the channel opening time. The largest transient occurs $1.1 \pm 0.17$ms before opening, has an amplitude of $5.1 \pm 1.6$ fA and an apparent duration of 300$\mu$s. However, the transient autocorrelation function indicates that its actual duration is shorter. The calculated equivalent charge displaced across the membrane is $4.7 \pm 2.5$ charges. Another current peak occurs 300$\mu$s before channel opening. The slow gating current component is assumed to represent conformational changes of stochastic nature while the transients, time locked to the channel opening, reflect transitions of deterministic nature. Simulation of gating models consisting of a pair of pathways leading to the open state, one of which includes stochastic and pre-open deterministic transitions and the other only stochastic transitions are shown to be consistent with experimental time histograms and gating current results. Models consisting of only stochastic transitions fail to do so.

**Tu-AM-H6**

**DETERMINATION OF SHAKER $K^+$ CHANNEL NUMBER AND GATING CHARGE IN INDIVIDUAL XENOPUS OOCYTES**
**((Sanjay K. Aggarwal and Roderick MacKinnon)) Department of Neurobiology, Harvard Medical School, Boston, MA 02115.**

A recombinant scorpion toxin (charybdotoxin isoform) was modified by introducing an extra cysteine residue on the "back side" of the toxin as identified by Stampe and Miller. $^3$H N-ethylmaleimide was linked to the free cysteine to yield a high-affinity radiolabeled ligand with properties similar to the unmodified toxin ($K_d$ = 160 pM, $k_{off}$ = 0.0014 $s^{-1}$). Shaker $K^+$ channels were expressed in Xenopus oocytes and toxin binding studies were carried out 1-7 days after RNA injection. Individual oocytes were incubated in radiolabeled toxin, washed, and then assayed by scintillation counting. Typically, Shaker $K^+$ channels express to a level of $10^{10}$ per oocyte. This assay enables us to measure gating current and, in the same oocyte, count receptors to determine the gating charge per toxin binding receptor.

**Tu-AM-H7**

**THE COMPONENTS OF *Shaker* $K^+$ CHANNEL GATING CURRENTS**
((E. Perozo, E. Stefani and F. Bezanilla)) Dept. of Physiology and Jules Stein Eye Inst., UCLA, and Dept. Mol. Biophysics, Baylor College of Medicine.

A kinetic and steady state analysis of high resolution gating currents was performed in cut-open oocytes expressing non-inactivating, non-conducting Shaker K channels (W434F H4-IR). The charge vs. potential (Q-V) curve revealed at least two distinct components of charge movement. The first component moves in the hyperpolarized region ($V_{½}$=-63 mV, z=2.4) and the second, with a larger apparent valence (z=5.), moves in a more depolarized region of potential ($V_{½}$ =-44 mV). A kinetic analysis of the gating current relaxations also revealed two distinct exponential decaying components. When the charge is analytically integrated, these kinetic components closely parallel the charge components described in the steady state. The first component corresponds to charge movement among deep closed states and correlates with the Cole-Moore shift. The second component corresponds to the events preceding the opening of the channel. The appearance of a pronounced rising phase in both, the ON and the OFF gating currents occurs at potentials in which the second component becomes predominant. These results cannot be explained with simple parallel models. The data were fitted with an 8 state sequential model in which the first series of charge movements carry less than 2 electronic charges per step (1.8, 1.2, 1.2, 1.2 and 0.9 $e_o$=electronic charges times fraction of the field). This first series of steps correlates with the first component of the gating currents. The following series, which correlates with the second component of the gating current, consists of two steps, the first carrying 3.5 $e_o$ and a final step leading to the open state carrying 0.35 $e_o$. Supported by USPHS grants GM 30376, and AR38970 and The Pew Charitable Trust.

**Tu-AM-H8**

**NOISE ANALYSIS OF GATING CURRENTS FROM *SHAKER* $K^+$ CHANNEL YIELDS INFORMATION ABOUT CHARGE COMPONENTS.**
((D. Sigg*, E. Stefani¶, F. Bezanilla*)) *Department of Physiology, UCLA, Los Angeles, CA 90024 and ¶Department of Physiology and Molecular Biophysics, Baylor College of Medicine, Houston TX.

The voltage-dependence of ion channel activation is the result of charge movement coupled to conformational transitions (gating charge). Non-stationary fluctuation analysis of gating currents from *Xenopus* oocytes injected with a non-conducting and non-inactivating variant of the *Shaker* $K^+$ channel reveals that at least some charge-carrying transitions occur as discrete "shots". The lack of a discernible slowly varying component in the autocovariance function indicates that the recording bandwidth of 8 kHz provides sufficient temporal resolution to extract useful kinetic information from comparisons between the ensemble mean and variance. For a pulse to -50 mV, there is a significant delay of the peak of the variance with respect to the peak of the mean, decreasing at depolarized potentials, indicating that the initial steps of activation consists of a series of fast transitions carrying little charge, followed by a finite number of discrete, correlated transitions. By fitting the plot of variance vs. mean to a parabolic equation, we obtained a lower estimate of 2.4 $e_o$ ($1.6 \times 10^{-19}$ Coul. times the fraction of the membrane field) for the largest transition charge. Based on these results and those of Schoppa et. al. (*Science* **255**: 1712, 1992), which estimated 12.4 $e_o$ of gating charge moved per activating channel, we conclude that the physical subunits that make up *Shaker* must, at some point in the activating process, act in concert, moving discrete "shots" of gating charge. Supported by USPHS GM30376 and AR38970.

**Tu-AM-H9**

STABLE EXPRESSION OF HUMAN KV1.3 POTASSIUM CHANNELS RESETS THE RESTING POTENTIAL OF CHO CELLS.
((R.J. Leonard, S.P. Stevens, and F. P. DeFarias)) Membrane Biochemistry & Biophysics, Merck Research Labs, Rahway, NJ 07095.

A cDNA clone encoding the human Kv1.3 potassium channel was stably expressed at high levels in CHO cells. The expressed currents resemble strongly those recorded from *Xenopus* oocytes injected with Kv1.3 cRNA, or from resting human T lymphocytes. Using conventional whole cell voltage clamp, the rate of inactivation of the $K^+$ current recorded either from injected oocytes or from transfected CHO cells is slower than that recorded from human T cells. However, such slow inactivation is routinely observed in perforated patch recordings from human T cells. One function ascribed to Kv1.3 in T lymphocytes is to stabilize the membrane potential, thereby regulating the $Ca^{2+}$ signalling critical for mitogenic stimulation. In agreement with this hypothesis, we find that heterologous expression of Kv1.3 changes the resting potential of CHO cells, setting it to the threshold for activation of Kv1.3. Inhibitors of Kv1.3, such as margatoxin or 4-aminopyridine, rapidly and reversibly depolarize transfected CHO cells to the potential observed in non-transformed cells. The combination of steep voltage-dependence of activation with slow and incomplete inactivation appears to confer the ability of the Kv1.3 channel to "clamp" the $V_m$ of its host cell within a narrow range.

**Tu-AM-H10**

THE ACTION OF 4-AMINOPYRIDINE ON THE ACTIVATING CONFORMATIONAL REARRANGEMENTS OF VOLTAGE-DEPENDENT *SHAKER* $K^+$ CHANNELS.
((Ken McCormack*, William Joiner and Stefan H. Heinemann)) Max-Planck-Institut für Experimetelle Medizin 11, Department of Physiology, Yale University, Max-Planck-Institut für biophysikalische Chemie 140.

We have examined the blocking action of 4-AP on both the ionic and gating currents of *Shaker* K+ channels using patch and two-microelectrode recordings. The data indicate that: i) The binding site for 4-AP is not accessible during resting closed states (at -100 mV), but becomes so from the internal side of the membrane upon activation. In addition, bound 4-AP becomes trapped within the protein upon returning to the resting closed state. ii) Voltage-dependent effects of 4-AP are consistent with a state-dependence of binding. When binding is equilibrated 4-AP does not decrease the activation or deactivation kinetics of the channels that open. Thus, channels open only when 4-AP is not bound. iii) 4-AP selectively blocks a slow component of on-charge movement at potentials where the channels begin to open and it speeds up the off-gating charge; 4-AP blocks a distinct conformational rearrangement of the channel protein associated with later stages of activation. iv) A larger percentage of the gating charge is blocked at potentials of lower rather than higher open probability. One explanation for this result is that different proportions of the channels traverse distinct kinetic pathways at the different potentials. v) The binding of 4-AP to a single site blocks all of the 4-AP-sensitive rearrangements suggesting that 4-AP blocks a concerted conformational transition. vi) In the presence of 4-AP both the kinetic and steady-state properties of the unblocked rearrangements are virtually symmetric in the forward and backward direction. This suggests that the charge moved from any conformational state to any neighboring transition state (in either the forward or backward direction) is roughly identical. vii) An allosteric model for the activation of these channels explains the action of 4-AP.

**Tu-AM-I1**

**PROPERTIES OF NONPLANAR HALOGENATED DODECAPHENYLPORPHYRINS EFFECTED BY ELECTRON WITHDRAWING SUBSTITUENTS.** ((K.K. Anderson,[1,2] J.D. Hobbs,[1] G.N. Ryba,[1] S.A. Majumder,[1,2] C.J. Medforth,[3] T.P. Forsyth,[3] K.M. Smith,[3] K. M. Kadish,[4] and J.A. Shelnutt[1,2]) [1]Fuel Science Department 6211, Sandia National Laboratories, Albuquerque, NM 87185-5800. [2]Department of Chemistry, University of New Mexico, Albuquerque, NM 87131. [3]Department of Chemistry, University of California, Davis CA 95616. [4]Department of Chemistry, University of Houston, Houston, TX 77204-5641.

**Conformational distortion of metalloporphyrins and the electron withdrawing capacity of the peripheral substituents play a role in determining the biological properties and function of tetrapyrrole cofactors of proteins. To understand these structural and electronic effects we used resonance Raman spectroscopy to examine the iron and nickel derivatives of a series of fluorinated dodecaphenylporphyrins ($DPPF_x$; x = 0,20,28,36) and dodecaphenylporphyrin with eight chlorine atoms substituted on the ortho position of the meso-phenyl rings ($DPPCl_8$). Molecular mechanics calculations show no differences in the structures of the fluorinated DPPs, implying differences in the spectra are primarily due to electron withdrawing effects. The frequency of two Raman lines, $\nu_4$ and $\nu_2$, show shifts to higher frequency in the series: $F_0<F_{20}<F_{28}<F_{36}$; therefore, these lines may be used as markers of electron-withdrawing capacity when conformation does not vary. Nickel and copper derivatives of octa(isopropyl-phenyl)porphyrin (MOIPPP) were used to further investigate the effect of the β-pyrrole phenyl substituents on the Raman spectra. NiOIPPP is found to be a mixture of planar and nonplanar conformers as has been previously noted for Ni octaethylporphyrin. Other structure-sensitive lines of NiOIPPP including $\nu_4$, $\nu_3$, and $\nu_2$ exhibit large shifts caused by the phenyl substituents.**

Supported by the U.S. Dept. of Energy Contract DE-AC04-94AL85000 and Associated Western Universities (KKA, JDH, SAM, LDS, and CJM ).

**Tu-AM-I2**

**AGGREGATION AND COMPLEXATION PROPERTIES OF NONPLANAR WATER-SOLUBLE OCTAACETIC ACID-TETRAPHENYLPORPHYRIN.**
((S.A. Majumder,[1,2] M. Miura,[3] J.D. Hobbs,[1] and J.A. Shelnutt[1,2]) *[1]Fuel Science Department 6211, Sandia National Laboratories, Albuquerque, NM 87185. [2]Department of Chemistry, University of New Mexico, Albuquerque, NM 87131. [3]Medical Department, Brookhaven National Laboratory, Upton, NY 11973.*

**Nonplanarity of porphyrin macrocycles in proteins may play a role in their function. The nickel derivative of the water-soluble, nonplanar porphyrin (2,3,7,8,12,13,17,18-octaacetic-acid-5,10,15,20-tetraphenylporphyrin (OAATPP) has been synthesized and its aqueous physical and chemical properties, including interactions with complexing agents, have been investigated using UV-visible absorption and resonance Raman spectroscopies. Red shifts of 16-36 nm in the major absorption bands relative to nickel octaethylporphyrin and tetraphenylporphyrin derivatives are indicative of a high degree of nonplanarity for NiOAATPP. Resonance Raman studies also indicate a nonplanar conformation for NiOAATPP by the downshifts in the frequencies of the structure-sensitive marker lines. At low pH (<3) or in 5M NaCl, planar octaacidporphyrins like Ni uroporphyrin (NiUroP) form π–π aggregates resulting in small characteristic upshifts in the structure-sensitive Raman lines. In contrast, NiOAATPP shows no significant changes in either the absorption or the Raman spectra; therefore the π–π aggregate formed by planar NiUroP does not form for NiOAATPP, most likely because of the steric difficulty in stacking this highly nonplanar and sterically hindered porphyrin. The complex between NiOAATPP and methylviologen (MV) shows minimal changes in the absorption spectrum in contrast with the strong π–π complex with NiUroP. However, the Raman spectrum of the NiOAATPP-MV complex shows downshifts in frequencies indicating interaction between the porphyrin and MV. Molecular modeling supports an *edge on* orientation between NiOAATPP and MV instead of the *flat* π–π interaction for NiUroP.** Supported by the U.S. DOE Contracts DE-AC04-94AL85000 and Associated Western Universities (SAM and JDH).

**Tu-AM-I3**

DETERMINANTS OF THE SPIN STATE OF THE RESTING STATE OF CYTOCHROME P450*cam*.
((D. Harris and G. H. Loew)), Molecular Research Institute, 845 Page Mill Road, Palo Alto, CA 94304.

The origin of the low-spin ground state of the substrate-free ferric resting state of cytochrome P450*cam* has been investigated with use of the combined techniques of restricted open-shell Hartree-Fock INDO/S calculations together with molecular dynamics. The presence of water as the heme-iron ligand, while resulting in a small energy separation of the S = 5/2 and 1/2 ferric heme spin states, is by itself insufficient to explain the experimentally observed low-spin resting state. However, the inclusion of the electrostatic field of the protein in the INDO/S Hamiltonian, using the optimized X-ray coordinates and electrostatic potential-derived partial charges found in AMBER, results in a low-spin resting state of cytochrome P-450*cam*. Molecular dynamic simulations of the optimized X-ray structure further support the role of the protein in modulating the spin state equilibrium. The dynamic motion of the heme unit is not sufficient to account for the predominance of the low-spin state, while the dynamic effect of the field of the protein favors the low-spin state. By contrast, in the camphor-bound cytochrome P450*cam*, the field of the protein does not reverse the high spin state found for the optimized X-ray structure of the heme unit. These results have revealed a heretofore unidentified role of the protein in modulating spin equilibrium, a property of the ferric heme unit that is central to the maintenance of the enzymatic function of the cytochrome P450s.

**Tu-AM-I4**

**ASSEMBLY OF SYMMETRICAL INTER-SPECIES HYBRIDS OF HUMAN AND SWINE HEMOGLOBIN IN VIVO AND IN VITRO.** ((M. J. Rao*, B. N. Manjula**, R. Kumar** and A. S. Acharya*,)) *Albert Einstein Col. of Med., Bronx, N.Y. and **DNX Corporation, Princeton, N.J.

In transgenic swines expressing human HbA, only one of the two anticipated interspecies hybrids, $^{H}\alpha_2^{P}\beta_2$, is present. In an attempt to gain insights into the absence of $^{P}\alpha_2^{H}\beta_2$ hybrid **in vivo**, we have now assembled both of these hybrids **in vitro** by alloplex intermediate pathway. The success in this **in vitro** assembly demonstrates the presence of complementarity between the respective pairs of the interspecies chains. The two hybrids are stable, and the parent species are not generated even when the two are mixed together. The interspecies hybrids are also not formed when HbA and swine Hb are mixed together, thus establishing the stability of all the four tetramers. On the other hand, when the hybrid $^{P}\alpha_2^{H}\beta_2$ is mixed with $^{H}\alpha$ chain at pH 6.0, nearly complete exchange of the $^{P}\alpha$ chain of the hybrid occurred in 24 hours resulting in the formation of HbA. But the hybrid, $^{H}\alpha_2^{P}\beta_2$ is refractory for the exchange reaction with $^{H}\beta$ chains. Accordingly, we speculate that the stability of the intradimer $\alpha_1\beta_1$ interface of $^{P}\alpha^{H}\beta$ dimer is very low and the presence of the complimentary native chains ($^{H}\alpha$ and $^{P}\beta$) during the assembly as in the **in vivo** studies permits the ready segregation of the transient interspecies dimers into native swine or human dimers, and hence the absence of $^{P}\alpha_2^{H}\beta_2$ hybrids **in vivo**. However, in absence of this segregation, two dimers interact to form new interdimer $P\alpha_1^{H}\beta_2$ interfaces. The generation of the interdimer interfaces either compensate for the lower stability of the $\alpha_1\beta_1$ interface or stabilizes this interface through long range communication. The latter situation facilitates the the formation of the interspecies hybrid $^{P}\alpha_2^{H}\beta 2$ **in vitro**. This molecular aspect contributes to the discrepancy in the results of the **in vivo** and **in vitro** studies.

**Tu-AM-I5**

NON-PLANAR DISTORTIONS OF NI(II)-OCTAETHYLTETRAPHENYLPORPHYRIN IN $CS_2$ PROBED BY RAMAN DISPERSION SPECTROSCOPY ((R. Schweitzer-Stenner[1], A. Stichternath[1], W. Dreybrodt[1], C. Medforth[2] and K.M. Smith[2])) [1]Inst. of Exp. Physics, Univ. of Bremen, 28359 Bremen, Germany and [2] Dep. of Chemistry, UC Davis, Davis, CA 95616, USA.

We have measured the polarized excitation profiles (REPs) of 23 Raman lines of Ni(II)-octaethyltetraphenylporphyrin in $CS_2$ (NiOETPP). The data cover the resonant regions of the Q- and B-bands. While all $A_{1g}$ and $A_{2g}$ lines (f.i. $\nu_2$, $\nu_4$, $\nu_{19}$, $\nu_{21}$) exhibit a significant dispersion of their depolarisation ratios (DPRs), the DPRs of the $B_{1g}$ and $B_{2g}$-lines (f.i. $\nu_{11}$, $\nu_{10}$, $\nu_{28}$) are either constant or only weakly dispersive. The data were analyzed by formulating the Raman tensor in terms of a perturbation approach, which explicitly considers the multimode contributions of the investigated lines. This yields vibronic coupling parameters depending on the symmetry of the porphyrin macrocycle. It turned out that the DPR-dispersions of the $A_{1g}$-lines result from a mixing of $A_{2g}$-type coupling into their Raman tensors, whereas mixing with $A_{1g}$-type coupling causes the DPR-dispersion of the $A_{2g}$-lines. This symmetry mixing result from out-of-plane distortions, which cause tilting ($B_{2u}$) and twisting ($B_{1u}$) of the pyrroles. The nearly constant DPRs of $B_{1g}$ and $B_{2g}$ modes suggest that $A_{1u}$ and $A_{2u}$ - distortions are less effective. Vibronic coupling parameters are larger than those of corresponding modes in Ni(II)-octaethylporphyrin, but smaller than the respective values in Ni(II)-porphin. This shows the strong influence of peripheral substituents on the vibronic properties of the macrocycle.

**Tu-AM-I6**

**DNA-METALLOPORPHYRIN π-π INTERACTIONS IN INTERCALATED COMPLEXES.** ((S.K.Subbarao[1,2], M.Miura[3], K.K.Anderson[1,2], J.D.Hobbs[1], J.A.Shelnutt[1,2])) [1]Fuel Science Department 6211, Sandia National Laboratories, Albuquerque, NM 87185 and [2]Department of Chemistry, University of New Mexico, Albuquerque, NM 87131. [3]Medical Department, Brookhaven National Laboratory, Upton, NY 11973.

**The interactions of metalloporphyrins intercalated into DNA has been investigated using dual-channel resonance Raman spectroscopy (RRS) and UV-visible absorption spectroscopy. The spectra of metalloporphyrin in the DNA complex have been compared with metalloporphyrin aggregates and π-π complexes. It is already well known that nickel(II) tetra(N-methylpyridyl)porphyrin ($TMePyP^{+4}$) intercalates into DNA at GC rich regions. In aqueous solution in the absence of DNA, $NiTMePyP^{+4}$ is a mixture of the 4-coordinate species and the 6-coordinate bis-aquo complex, but DNA-bound $NiTMePyP^{+4}$ is entirely in the 4-coordinate form. We have used RRS to further investigate the nature of this DNA-bound 4-coordinate complex. Shifts in the frequencies of the structure-sensitive Raman lines of DNA-bound, 4-coordinate Ni- and $CuTMePyP^{+4}$ relative to the unbound 4-coordinate species were obtained for calf-thymus DNA. These shifts are compared to the complex-induced shifts for complexes of the metal porphyrin with 1,10-phenanthroline (phen), 1,7-phen, and 5-Cl-1,10-phen. The shifts for the salt-induced aggregates were also obtained and compared with the DNA-porphyrin complex. Shifts in these model π–π complexes and aggregates are of similar magnitude but distinct from those of the DNA complex. DNA complexes with cationic β-pyrrole substituted metalloporphyrins will also be discussed.**

Supported by the U.S. Department of Energy Contract DE-AC04-94DP85000 and Associated Western University Fellowships (SKS, KKA, JDH).

Tu-AM-I7

RAMAN SPECTROSCOPY OF LIGAND BINDING TO MYOGLOBIN AT HIGH PRESSURE. (( A. Schulte, C. Williams)) Department of Physics and Center for Research in Electro-Optics and Lasers, University of Central Florida, Orlando, FL 32817.

The effect of high pressure on the resonance Raman spectrum of (horse) carbonmonoxymyoglobin was measured using excitation at 457 nm. By monitoring the oxidation state marker bands ($\nu_4$ : 1374 $cm^{-1}$ for MbCO and 1356 $cm^{-1}$ for Mb) we show that there is a significant increase of the band at 1374 $cm^{-1}$ relative to that at 1356 $cm^{-1}$ upon raising the pressure from 1 atm to 180 MPa. This is consistent with a negative activation volume of MbCO. We explore conformational transitions of the protein by performing experiments with cyclic pressure changes.

* Supported by NSF, Grant No. MCB-9305711.

Tu-AM-I8

MULTI-VARIABLE APPROACH TO THE DESIGN OF CROSSLINKED HEMOGLOBINS ((Kenneth W. Olsen, Liang Zhao, Yaguo Zheng, Mary F. Reifsteck, Frank L. White and K. Sujatha)) Department of Chemistry, Loyola University, 6525 N. Sheridan Rd., Chicago, IL 60626.

Computer-aided molecular design is being used to propose new crosslinking reagents for human hemoglobin. In this design process, molecular dynamics calculations have been used to assess the flexibility of both the reagent and the reaction site on the protein. Long, hydrophilic diaspirin reagents have been designed to crosslink different hemoglobin tetramers together or to crosslink hemoglobin to protective enzymes, such as catalase or superoxide dismutase. Multilinkers, which react with the protein at more than two sites, are being made to modify single hemoglobin tetramers and to form hemoglobin octamers. Reagents designed to react between tetramers as they are oriented in the crystalline state are also being used. These reagents offer the possibility of forming complexes that cannot be made in solution. Finally, molecular dynamics simulations are being used to predict the effects of crosslinking on protein flexibility. (Supported in part by a grant from the Research Corporation.)

Tu-AM-I9

**FLUORINATED IRON DODECAPHENYLPORPHYRINS AS ALKANE-OXIDATION CATALYSTS.** ((M. C. Showalter, K. E. Erkkila, J. A. Shelnutt)) *Fuel Science Department 6211, Sandia National Laboratories, Albuquerque, NM 87185-5800.*

**Computer-aided molecular design methods are being used in conjunction with catalytic activity testing to develop biomimetic iron-porphyrin catalysts that incorporate the structural features responsible for enzyme catalysis. In this work the focus is on models of cyctochromes P450. A series of fluorinated iron dodecaphenyporphyrins ($FeDPPF_x$, where x = 0, 20, 28, and 36) has been synthesized, characterized, and tested for catalytic activity. Desired molecular design features in these catalysts include a substrate binding cavity common to the entire series and increased electron-withdrawing ability of the porphyrin ligand across the series as the number of fluorine substituents increases. These porphyrins were tested as catalysts in the oxidation of light alkanes, including isopentane, to alcohols. Catalytic activity was found to increase with the number of fluorine substituents regardless of whether iodosylbenzene or $O_2$ was used as the oxidant. This increase in activity is attributed solely to the electronic effect of the fluorine substituents because molecular modeling and spectroscopic studies show that replacing hydrogen with fluorine on the phenyl substituents does not alter the conformation of the porphyrin macrocycle. In addition, these catalysts, which have a substrate binding cavity, show novel selectivities in some reactions. Future work will involve using the insights gained thus far to continue designing catalysts which are predicted to be more active and selective.**

Supported by United States Department of Energy Contract DE-AC04-94AL85000.

## SEVEN HELIX RECEPTORS

Tu-PM-Sym-1

CONSTITUTIVE ACTIVATION OF RHODOPSIN AS A MOLECULAR MECHANISM OF DISEASE. ((D.D. Oprian)) Dept. of Biochemistry, Brandeis University, Waltham, MA 02254.

We have identified four different amino acid residues in the visual pigment rhodopsin that when mutated cause constitutive activation of the apoprotein opsin. These amino acids are $Gly^{90}$, $Glu^{113}$, $Ala^{292}$, and $Lys^{296}$. In each case, activation of the mutant protein appears to result from the disruption of a salt bridge between $Glu^{113}$ and $Lys^{296}$. Mutations at three of these positions ($Gly^{90} \rightarrow$ Asp, $Ala^{292} \rightarrow$ Glu, and $Lys^{296} \rightarrow$ Glu or Met) have been found in the diseases congenital night blindness and retinitis pigmentosa. We speculate that the unregulated activity of the mutant receptors is causing disease in patients with these mutations. We are currently designing active site-directed inactivators which selectively target the constitutively active mutant receptors.

Tu-PM-Sym-2

LIGAND BINDING DOMAINS OF G PROTEIN COUPLED RECEPTORS. ((C.D. Strader, T.M. Fong, M.R. Candelore, and M.R. Tota)) Merck Research Labs, Rahway, NJ 07065.

Receptors whose mechanism of action is mediated through the activation of G proteins share structural, as well as functional, similarities. These receptors consist of seven hydrophobic domains, postulated to form transmembrane helices, connected by hydrophilic loops. Site-directed mutagenesis of the ß-adrenergic receptor has shown that the ligand binding domain is contained within the transmembrane core of the receptor, with most of the binding energy provided by an ion pair formed between the amine group of the catecholamine ligand and the carboxylate side chain of Asp113 in the third transmembrane domain of the receptor. G protein activation is triggered by interactions of the catechol ring of the ligand with residues in helices 5 and 6 of the receptor. In contrast to the relatively compact ligand binding domain of the catecholamine receptors, the undecapeptide substance P binds to both the transmembrane and extracellular regions of the NK1 neurokinin receptor. Small molecule antagonists of this receptor have recently been described, and specific interactions between these antagonists and residues in the transmembrane domain of the NK1 receptor have been identified. The similarity in the location of the non-peptide antagonist binding site in the NK1 receptor with that of the biogenic amine binding site in the ß-adrenergic receptor suggests the existance of a generally conserved binding site for small molecules in the transmembrane domains of G protein coupled receptors.